ARTICLE

Lymph node fibroblastic reticular cells regulate differentiation and function of CD4 T cells via CD25

Dongeon Kim[1,2,4]*, Mingyo Kim[1,5]*, Tae Woo Kim[1,3]*, Yong-ho Choe[5]*, Hae Sook Noh[5], Hyun Min Jeon[5], HyunSeok Kim[1], Youngeun Lee[1], Gayeong Hur[1,6], Kyung-Mi Lee[7], Kihyuk Shin[8,9], Sang-il Lee[5], and Seung-Hyo Lee[1,2,3]

Lymph node fibroblastic reticular cells (LN-FRCs) provide functional structure to LNs and play important roles in interactions between T cells and antigen-presenting cells. However, the direct impact of LN-FRCs on naive CD4^{+} T cell differentiation has not been explored. Here, we show that T cell zone FRCs of LNs (LN-TRCs) express CD25, the α chain of the IL-2 receptor heterotrimer. Moreover, LN-TRCs *trans*-present IL-2 to naive CD4^{+} T cells through CD25, thereby facilitating early IL-2–mediated signaling. CD25-deficient LN-TRCs exhibit attenuated STAT5 phosphorylation in naive CD4^{+} T cells during T cell differentiation, promoting T helper 17 (Th17) cell differentiation and Th17 response-related gene expression. In experimental autoimmune disease models, disease severity was elevated in mice lacking CD25 in LN-TRCs. Therefore, our results suggest that CD25 expression on LN-TRCs regulates CD4^{+} T cell differentiation by modulating early IL-2 signaling of neighboring, naive CD4^{+} T cells, influencing the overall properties of immune responses.

Introduction

LNs are secondary lymphoid organs that facilitate the interaction between APCs and their cognate T cells and promote the initiation of adaptive immune responses (Gretz et al., 1996; Stoll et al., 2002). LN stromal cells (LNSCs), which play a critical role in LN structure, are a nonhematopoietic heterogeneous population that can be classified based on the expression of the surface markers CD31 (PECAM-1) and gp38 (podoplanin). LNSCs consist of fibroblastic reticular cells (CD31−gp38+), blood vessel endothelial cells (CD31+gp38−), lymphatic endothelial cells (LECs, CD31+gp38+), follicular dendritic cells (CD31−gp38+/−), and undefined stroma (Link et al., 2007). Recent studies have characterized LNSCs as modulators of adaptive immune responses (Malhotra et al., 2012), as they interact with T cells, B cells, and dendritic cells (DCs; Dubrot et al., 2014).

T cell zone fibroblastic reticular cells of LNs (LN-TRCs) are a main population of nonhematopoietic stromal cells (Glegg et al., 1953) and represent a key cellular component providing structural and microenvironmental support for adaptive immune responses (Sixt et al., 2005). TRCs express extracellular matrix components to form a dense reticular network and facilitate the migration of lymphocytes and DCs (Gunn et al., 1998; Katakai et al., 2004). In addition, these cells produce the chemokines CCL19 and CCL21 to attract CCR7-expressing T cells and maintain homeostasis of naive T cells (Link et al., 2007). Activation of naive CD4^{+} T cells by antigen-bearing DCs occurs in direct contact with the TRC network to initiate immune responses (Bajenoff et al., 2006; Katakai et al., 2004). The TRC network provides a track on which T cells move, and because DCs are also found within the same stromal network, this offers an opportunity for T cells to scan DCs for specific antigens. However, it remains unknown whether these TRCs are actively involved in T cell activation and/or differentiation and, thus, the initiation of adaptive immune responses.

IL-2 influences various lymphocyte subsets during cell division, immune responses, cell death, and homeostasis (Morgan et al., 1976). *Trans*-presentation of IL-2 can occur in a manner similar to that of IL-15 (Wuest et al., 2011), which is mediated by the IL-15 receptor α chain (IL-15Rα; Dubois et al., 2002). IL-2R consists of three glycoprotein chains: α (IL-2Rα; CD25), β (IL-2Rβ; CD122), and common γ (γc; CD132; Minami et al., 1993).

[1]Graduate School of Medical Science and Engineering, Korea Advanced Institute of Science and Technology, Daejeon, South Korea; [2]Biomedical Science and Engineering Interdisciplinary Program, Biomedical Research Center, Korea Advanced Institute of Science and Technology, Daejeon, South Korea; [3]KAIST Institute for the BioCentury, Department of Biological Sciences, Korea Advanced Institute of Science and Technology, Daejeon, South Korea; [4]VA Palo Alto Health Care System, Stanford University School of Medicine, Stanford, CA; [5]Division of Rheumatology, Department of Internal Medicine and Institute of Health Science, Gyeongsang National University School of Medicine and Gyeongsang National University Hospital, Jinju, South Korea; [6]R&D Division, GenoFocus Inc., Daejeon, South Korea; [7]Department of Biochemistry and Molecular Biology, Korea University College of Medicine, Seoul, South Korea; [8]Department of Dermatology, Pusan National University Yangsan Hospital, Yangsan, South Korea; [9]Research Institute for Convergence of Biomedical Science and Technology, Pusan National University Yangsan Hospital, Yangsan, South Korea.

*D. Kim, M. Kim, T.W. Kim, and Y.-h. Choe contributed equally to this paper.   Correspondence to Seung-Hyo Lee: sl131345@kaist.ac.kr;   Sang-il Lee: goldgu@gnu.ac.kr; Kihyuk Shin: teriakiller@hanmail.net.

Although CD25 binds to IL-2 with low affinity and does not have signaling ability, surface expression of CD25 sensitizes neighboring T cells to low concentrations of IL-2 by capturing and presenting the cytokine first to CD122 and then recruiting CD132 to form the high-affinity trimeric IL-2R (Wang et al., 2005). The association of CD122 with CD132 induces signal transduction through heterodimerization of their cytoplasmic domains (Nakamura et al., 1994), leading to activation of JAK1 and JAK3 and subsequent phosphorylation of STAT5 (Leonard et al., 1999). IL-2 has crucial roles in the fate decisions of naive CD4^{+} T cells, resulting in their differentiation into distinct T helper (Th) cell subsets (Boyman and Sprent, 2012; Yamane and Paul, 2012). Specifically, IL-2 promotes Th1 cell differentiation via induction of T-bet (Liao et al., 2011), and Th2 cell differentiation requires IL-2–mediated activation of STAT5 (Le Gros et al., 1990; Zhu et al., 2010). In contrast, the IL-2-STAT5 pathway inhibits Th17 cell differentiation (Laurence et al., 2007).

Here, we investigated the regulation of CD4^{+} T cell differentiation into Th effector lineages by LN-TRCs for the first time. To identify molecular communicators involved in the regulation of CD4^{+} T cell function, we carried out flow cytometry to assess the expression of cytokine receptors on the surface of LN-TRCs and found that LN-TRCs specifically express only the CD25 subunit of the IL-2 receptor. Therefore, LN-TRCs can present IL-2 to neighboring, naive CD4^{+} T cells in a *trans*-presentation manner via CD25, thereby facilitating early IL-2–mediated signaling and affecting differentiation of CD4^{+} T cells. This *trans*-presentation augments STAT5 phosphorylation during the response of naive CD4^{+} T cells to IL-2. Conversely, CD25-deficient LN-TRCs promote Th17 cell differentiation via the reduced IL-2 signaling to naive CD4^{+} T cells ex vivo and exacerbate phenotypes of experimental autoimmune encephalomyelitis (EAE), an animal model of multiple sclerosis (MS); experimental psoriasis; and antigen-induced arthritis (AIA), an animal model of rheumatoid arthritis (RA), all of which are driven by Th17 cells, in vivo. These results suggest that optimizing cross-presentation of IL-2 by CD25 on LN-TRCs could be a candidate strategy to improve autoimmune diseases caused by pathogenic Th17 cells.

Results

LN-TRCs express only the CD25 receptor for IL-2 and do not respond to IL-2

To assess the direct influence of LN-TRCs on T cell–mediated immunity, we initially isolated primary LNSCs from cultured LN cells of C57BL/6J WT mice. LN-TRCs were sorted by FACS from CD45-free stromal cell–enriched fractions of LNs according to their expression of gp38 and lack of CD31. The purity of LN-TRCs was ≥95% after sorting (Fig. 1 A). A previous study reported that TRCs are essential for T cell homeostasis and enhance the survival of naive CD4^{+} T cells (Link et al., 2007). Accordingly, we examined whether sorted LN-TRCs enhanced survival of naive CD4^{+} T cells in the absence or presence of antibody stimulation. We observed that naive CD4^{+} T cells cocultured with LN-TRCs showed increased viability compared with naive CD4^{+} T cells cultured alone, even in the absence of antibody stimulation (Fig. S1 A), indicating that some factors provided by LN-TRCs

contribute to T cell survival. In addition, to determine whether naive CD4^{+} T cells are dependent on LN-TRCs for proliferation, we evaluated the cell division of CFSE-labeled naive CD4^{+} T cells under culture conditions with or without LN-TRCs in the presence of antibody stimulation. The proliferation of CD4^{+} T cells was significantly increased in the presence of LN-TRCs, compared with CD4^{+} T cells cultured alone (Fig. S1 B). We next examined the possible involvement of LN-TRCs in CD4^{+} T cell differentiation. To this end, naive CD4^{+} T cells were cultured alone or with LN-TRCs in the presence of antibody stimulation. Subsequently, the concentration of signature Th cell cytokines in culture supernatants was measured. CD4^{+} T cells cocultured with LN-TRCs generally secreted higher amounts of the Th1 cytokine IFN-γ, Th2 cytokine IL-4, and Th17 cytokine IL-17A compared with T cells cultured alone (Fig. S1 C), but the ratio of cytokine production regardless of the presence of LN-TRCs was not different. These results show that LN-TRCs significantly enhance survival and proliferation of CD4^{+} T cells, suggesting that LN-TRCs influence the function of naive CD4^{+} T cells.

The potential contribution of LN-TRCs to the differentiation of naive CD4^{+} T cells remains largely unexplored. Previous studies reported that TRCs are in contact with naive CD4^{+} T cells, and the TRC network within the LN paracortex facilitates access of naive CD4^{+} T cells to the paracortex (Bajenoff et al., 2006; Katakai et al., 2004). Because cell–cell contact between LN-TRCs and naive CD4^{+} T cells occurs in the LN paracortex, we hypothesized that cellular communication between LN-TRCs and T cells might contribute to naive CD4^{+} T cell differentiation. To explore the possibility of molecular communication between these cells, we first screened immunologically relevant receptors on fleshly isolated LN-TRCs (Fig. S2). The initial screening results revealed that LN-TRCs express CD25, a component of IL-2R. To confirm the expression of CD25, LN-TRCs were isolated from WT or CD25-deficient mice, and expression of IL-2R subunits was assessed. As shown in Fig. 1 B, LN-TRCs express CD25 but not CD122 or CD132. In addition, CD25 expression was confirmed in LN-TRCs from WT mice, but not CD25-deficient mice, by Western blot analysis (Fig. 1 C). Because IL-2–mediated signaling is achieved through heterodimerization of the CD122 and CD132 cytoplasmic domains (Nakamura et al., 1994), and our results showed that LN-TRCs only express CD25, we reasoned that LN-TRCs are not able to respond to exogenous IL-2. As expected, STAT5 phosphorylation was not detected in WT or CD25-deficient TRCs, whereas phosphorylated STAT5 was observed in naive CD4^{+} T cells, which express CD122 and CD132, when treated with recombinant IL-2 (Fig. 1 D). Taken together, these results indicate that LN-TRCs express the IL-2R component CD25 on the cell surface but do not respond to IL-2, suggesting that CD25-expressing TRCs play other roles in the T cell zone of the LN paracortex.

LN-TRCs *trans*-present IL-2 to naive CD4^{+} T cells through CD25

Because we observed that LN-TRCs expressed only CD25 and thus cannot mediate IL-2 signaling, we considered the possibility that CD25 on LN-TRCs affects neighboring cells, in particular, naive CD4^{+} T cells. Because CD25 is known to present receptor-
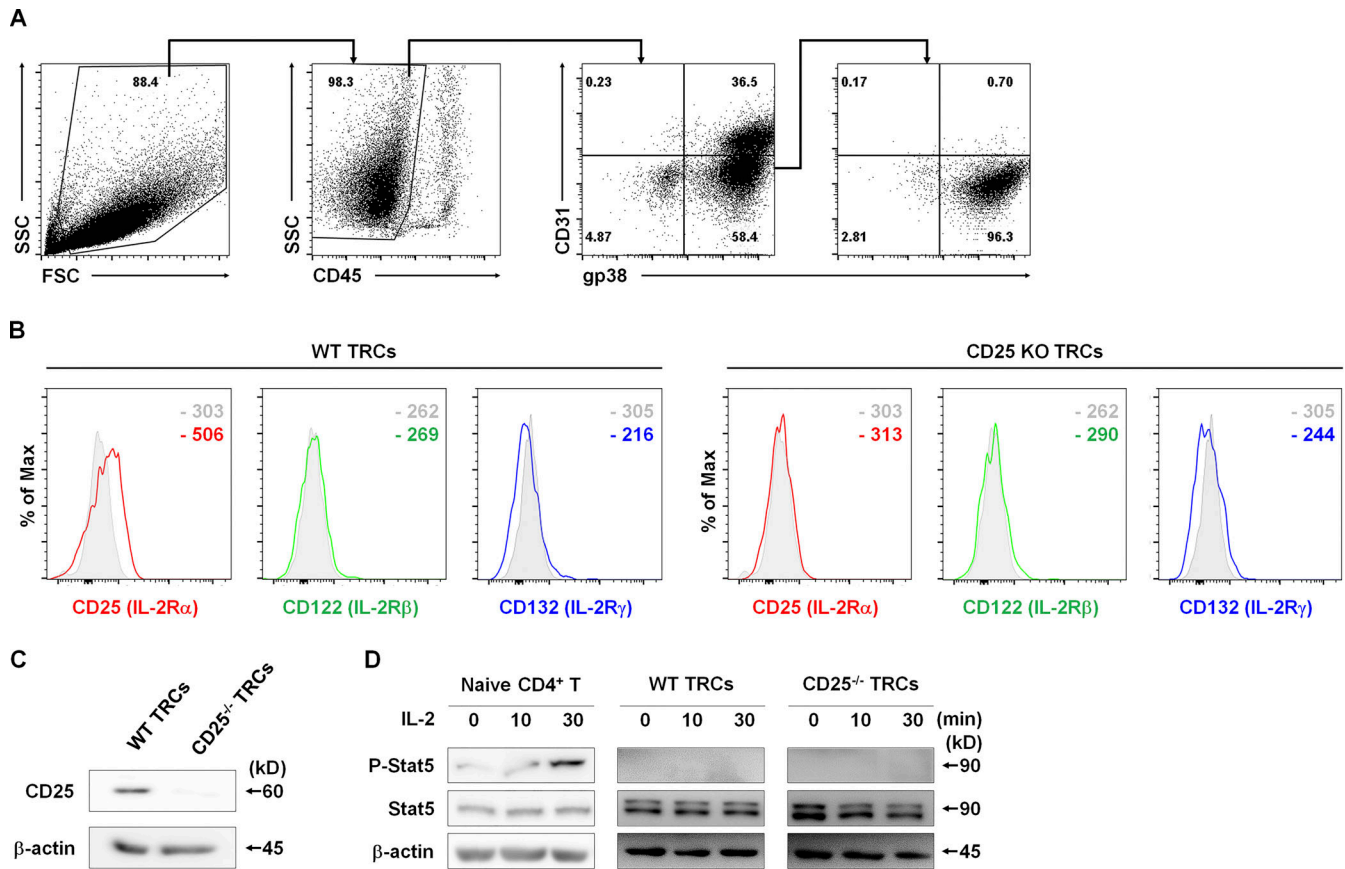
Figure 1. LN-TRCs express only CD25 and cannot induce IL-2–mediated signaling. (A) Representative flow cytometry sorting strategy for the isolation of TRCs from 5-d cultured LNSCs. LN-TRCs were isolated using a FACS Aria cell sorter. **(B)** Flow cytometry histograms show the mean fluorescence intensity of IL-2R subunits on TRCs. Gray histograms represent isotype control. **(C)** Expression of CD25 in WT or CD25-deficient TRCs was examined by Western blot analysis. β-Actin was used as a loading control. **(D)** Phosphorylation of STAT5 in WT or CD25-deficient TRCs after treatment with rIL-2 (20 ng/ml) at the indicated time points. STAT5 phosphorylation in naive CD4+ T cells is a positive control, and β-actin is a loading control. Data are representative of three independent experiments.

bound IL-2 to neighboring cells (Eicher and Waldmann, 1998) in a manner similar to the *trans*-presentation of IL-15 by IL-15Rα (Dubois et al., 2002), we assessed whether CD25 on LN-TRCs *trans*-presents IL-2 captured from the extracellular environment to neighboring naive CD4+ T cells. After treatment with rIL-2, we observed increased phosphorylation of STAT5 in naive CD4+ T cells when cocultured with WT TRCs, whereas STAT5 phosphorylation was not significantly enhanced in T cells cocultured with CD25-deficient TRCs (Fig. 2 A). To confirm the *trans*-presentation of IL-2 by CD25 on LN-TRCs, we performed flow cytometric analysis under the same experimental conditions. Phosphorylation of STAT5 was significantly increased in naive CD4+ T cells cocultured with WT TRCs (Fig. 2 B, left), but not when cocultured with CD25-deficient TRCs (Fig. 2 B, right). We next conducted immunofluorescence microscopy to further confirm the enhanced proximal IL-2 signaling and visualize nuclear translocation of phosphorylated STAT5. Nuclear translocation of phosphorylated STAT5 was clearly enhanced in naive CD4+ T cells cocultured with WT TRCs, but not after coculture with CD25-deficient TRCs (Fig. 2 C). Thus, these data indicate that CD25 on LN-TRCs enhances IL-2–induced signaling in naive CD4+ T cells through *trans*-presentation.

CD25 deficiency on LN-TRCs results in Th17 cell differentiation

IL-2 induces naive CD4+ T cell differentiation into either Th1 or Th2 cells and inhibits Th17 cell differentiation (Boyman and Sprent, 2012; Cote-Sierra et al., 2004; Laurence et al., 2007; Shi et al., 2008). Thus, we sought to determine whether the differentiation of naive CD4+ T cells is regulated by IL-2 *trans*-presented by LN-TRCs. To this end, we first assessed the levels of lineage-specific transcription factors (TFs) after coculture of naive CD4+ T cells with WT or CD25-deficient TRCs in the presence of antibody stimulation. The expression levels of the Th1- and Th2-specific TFs, T-bet and GATA3, were increased; however, the Th17-specific TF, RORγt (Ivanov et al., 2006), was relatively reduced in CD4+ T cells cocultured with WT TRCs compared with coculture with CD25-deficient TRCs (Fig. 3 A), suggesting that coculture with CD25-deficient TRCs promotes differentiation of Th17 cells ex vivo. To further investigate the effect of CD25 deficiency in LN-TRCs on Th17 cell differentiation, we examined the production of representative Th1, Th2, and Th17 cytokines after coculture with WT or CD25-deficient TRCs during antibody stimulation. Coculture with CD25-deficient TRCs significantly increased the secretion of IL-17A and reduced IFN-γ and IL-4 production by CD4+ T cells
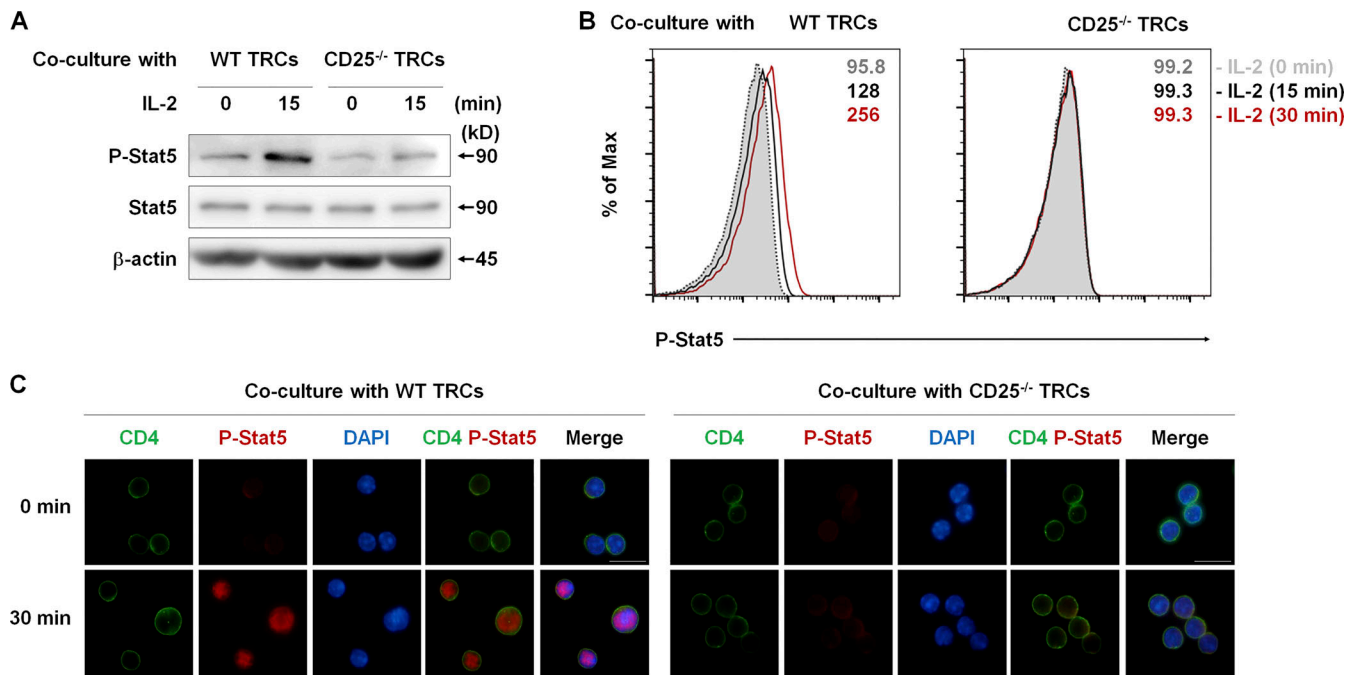
Figure 2. LN-TRCs *trans*-present IL-2 to CD4+ T cells through CD25. (A) STAT5 phosphorylation in naive CD4+ T cells cocultured with WT or CD25-deficient TRCs was assessed by Western blot analysis after 15-min treatment with rIL-2 (20 ng/ml). Total STAT5 and β-actin are shown as controls. **(B)** Representative flow cytometric histograms of STAT5 phosphorylation (P-Stat5) in naive CD4+ T cells cocultured with WT or CD25-deficient TRCs after treatment with rIL-2 (20 ng/ml) for the indicated time points. Mean fluorescence intensity is shown as a number. **(C)** STAT5 phosphorylation in naive CD4+ T cells cocultured with WT or CD25-deficient TRCs detected by immunocytochemical analysis after 30-min treatment with rIL-2 (20 ng/ml). Scale bar = 10 μm. Data are representative of three independent experiments.

compared with coculture with WT TRCs (Fig. 3 B). We also observed that the frequency of IL-17A–producing CD4+ T cells was markedly increased, while that of IFN-γ– and IL-4–producing CD4+ T cells decreased in coculture with CD25-deficient TRCs (Fig. 3 C). To further prove *trans*-presentation of IL-2 by TRCs in a cell–cell contact manner, we cocultured those cells in a *trans*-well system, and observed the frequency of IFN-γ, IL-4, and IL-17A production by CD4+ T cells was not different regardless of CD25 expression by TRCs (Fig. 3 D). Thus, these results demonstrate that CD25-deficient TRCs are not able to *trans*-present IL-2 to naive CD4+ T cells when IL-2 is present in the milieu, suggesting that CD25 deficiency on LN-TRCs enhances Th17 cell differentiation, which is caused by reduced IL-2 reactivity of naive CD4+ T cells.

IL-2 has been identified as a T cell growth factor involved in promoting T cell proliferation and survival (Bamford et al., 1994; Gillis and Smith, 1977; Schluns and Lefrancois, 2003). Accordingly, we investigated whether CD25 on LN-TRCs contributes to the survival of naive CD4+ T cells. Coculture with WT TRCs enhanced the survival of naive CD4+ T cells ex vivo, and remarkably, CD25-deficient TRCs also increased CD4+ T cell survival to a level similar to that induced by WT TRCs, even without any stimulation (Fig. S3 A). Thus, LN-TRCs might provide sufficient conditions for the survival of T cells independently of CD25 expression. Next, to investigate whether CD25 expression on LN-TRCs contributes to the proliferation of naive CD4+ T cells, we cocultured CFSE-labeled naive CD4+ T cells with WT or CD25-deficient TRCs in the presence of antibody stimulation.

The proliferation of CD4+ T cells was strongly enhanced by coculture with TRCs, regardless of CD25 expression (Fig. S3 B). Previous studies have also described T cell activation as an important step in the course of the immune response (Zaffran et al., 2001), and T cells are morphologically changed during activation (Wulfing et al., 1998). Thus, to determine whether activation of naive CD4+ T cells depends on CD25 expression on TRCs, we performed flow cytometric analysis to evaluate morphological changes of naive CD4+ T cells. The size and granularity of naive CD4+ T cells were unchanged before stimulation, and both parameters markedly increased after antibody stimulation (Fig. S3 C, left). More importantly, both the size and granularity of CD4+ T cells cocultured with TRCs were significantly increased compared with T cells alone with stimulation, regardless of CD25 expression on TRCs (Fig. S3 C, middle and right). Taken together, although important for T cell polarization, CD25 expression on LN-TRCs is not significantly associated with survival, proliferation, or activation of in vitro–stimulated CD4+ T cells.

CD25 deficiency increases EAE severity and Th17 responses in vivo

Thus far, our results show that coculture with CD25-deficient TRCs promotes the differentiation of naive CD4+ T cells into Th17 cells ex vivo. Because the roles of Th17 cells have been established in autoimmune conditions such as MS, psoriasis, and RA (Fletcher et al., 2010b; Sutton et al., 2006; Waite and Skokos, 2012; Yang et al., 2014), we next investigated whether CD25
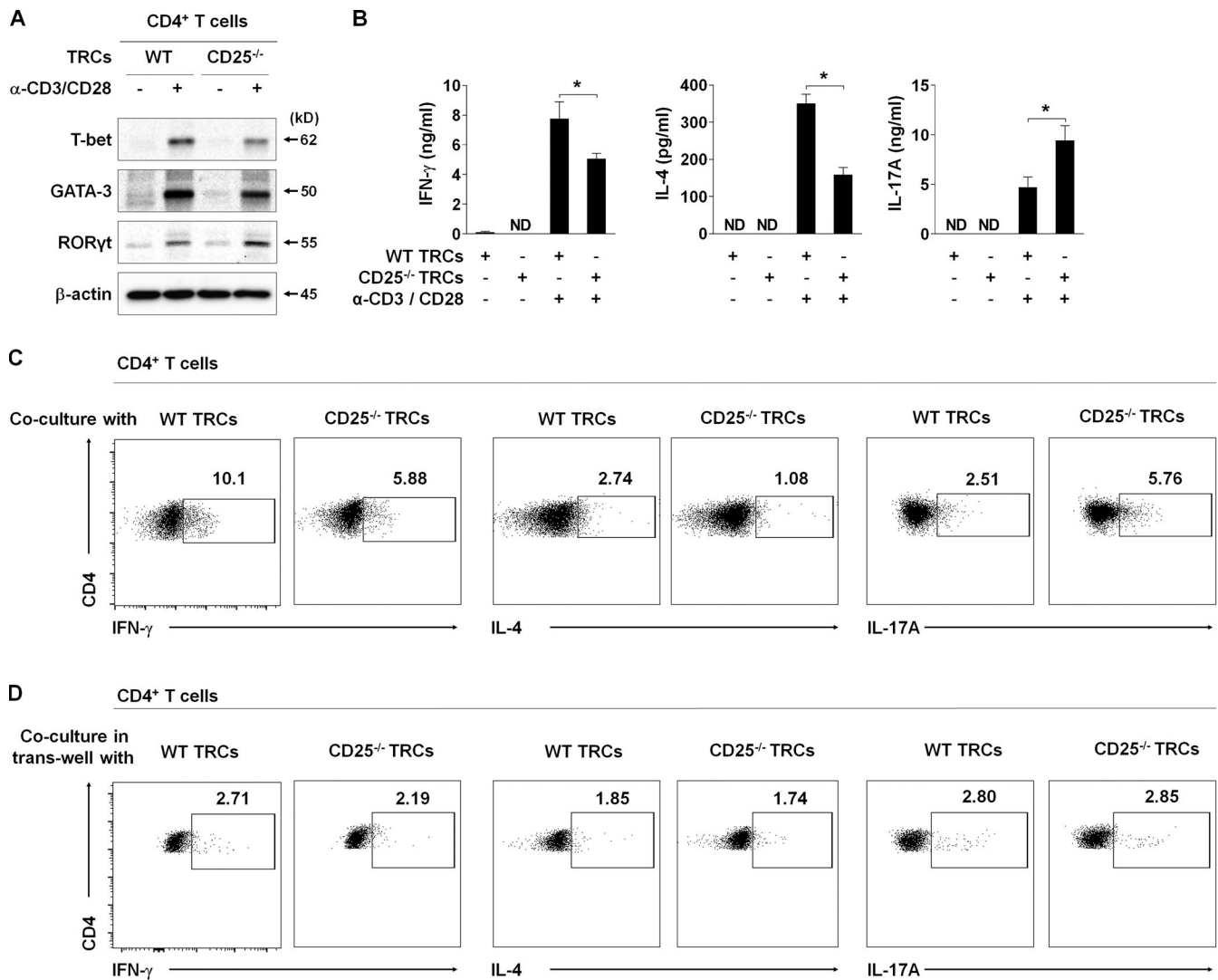
Figure 3. **CD25 deficiency on TRCs promotes in vitro Th17 differentiation.** Purified, naive CD4$^+$ T cells (2×10^5) were cocultured with or without WT or CD25-deficient TRCs (2×10^4) with irradiated APCs (1×10^5) in the presence or absence of soluble anti-CD3 and CD28 antibodies (3 and 1 µg/ml) for 72 h. **(A)** The expression of TFs (T-bet for Th1 cells, GATA-3 for Th2 cells, and RORγt for Th17 cells) in CD4$^+$ T cells cocultured with WT or CD25-deficient TRCs was detected by Western blot analysis. β-Actin is shown as a loading control. **(B)** Cytokine production (IFN-γ for Th1 cells, IL-4 for Th2 cells, and IL-17A for Th17 cells) in culture supernatants was quantified by ELISA. ND, not detectable; *, P < 0.05 compared with antibody-stimulated CD4$^+$ T cells cultured with WT TRCs or CD25-deficient TRCs. Error bars indicate the mean ± SEM (*n* = 5 per each group). **(C)** Representative flow cytometric plots of intracellular IFN-γ$^+$, IL-4$^+$, and IL-17A$^+$ cells in the CD4$^+$ T cell population. **(D)** Representative flow cytometric plots of intracellular IFN-γ$^+$, IL-4$^+$, and IL-17A$^+$ cells in the CD4$^+$ T cell population cultured in a *trans*-well system. Data are representative of three independent experiments.

deficiency enhances in vivo Th17 cell differentiation and subsequently exacerbates inflammatory responses during EAE. For this, we first assessed the kinetics of CD25 expression on LN-TRCs during the course of EAE induction, as it is possible that the dynamic expression of CD25 might control the differentiation of naive CD4$^+$ T cells. After induction of EAE in WT mice, inguinal LNs (iLNs) were harvested at designated time points to examine the expression of CD25 on LN-TRCs and IL-17A–producing CD4$^+$ cells (Fig. 4 A). LN-TRCs from mice with induced EAE showed reduced CD25 expression compared with TRCs from healthy mice on days 2, 5, 7.5, 9, and 14 (Fig. 4 B). Importantly, this decrease in CD25 was apparent as early as day 2. Subsequently, the population of IL-17A–producing CD4$^+$ T cells was increased on day 5 and reached the highest after the

second immunization, on day 7.5 (Fig. 4, C and D). Again, the population of IL-17A–positive CD4$^+$ T cells was decreased after the restoration of CD25 expression on TRCs (Fig. 4 D). Collectively, these results suggest the decrease of CD25 expression on LN-TRCs precedes the onset of EAE, and it might force Th17 cell–dominant differentiation.

Next, we adoptively transferred naive CD4$^+$ T cells from WT mice into either CD25/recombinase activating gene-1 (Rag-1) double-deficient (CD25$^{-/-}$RAG-1$^{-/-}$) or Rag-1 deficient (RAG-1$^{-/-}$) mice and induced EAE. Compared with CD25-sufficient RAG-1$^{-/-}$ recipients, CD25$^{-/-}$RAG-1$^{-/-}$ recipients, which have CD25-deficient TRCs, developed more severe EAE phenotypes (Fig. S4 A). Moreover, CD25$^{-/-}$RAG-1$^{-/-}$ recipients showed a significantly higher incidence of the disease compared with RAG-1$^{-/-}$
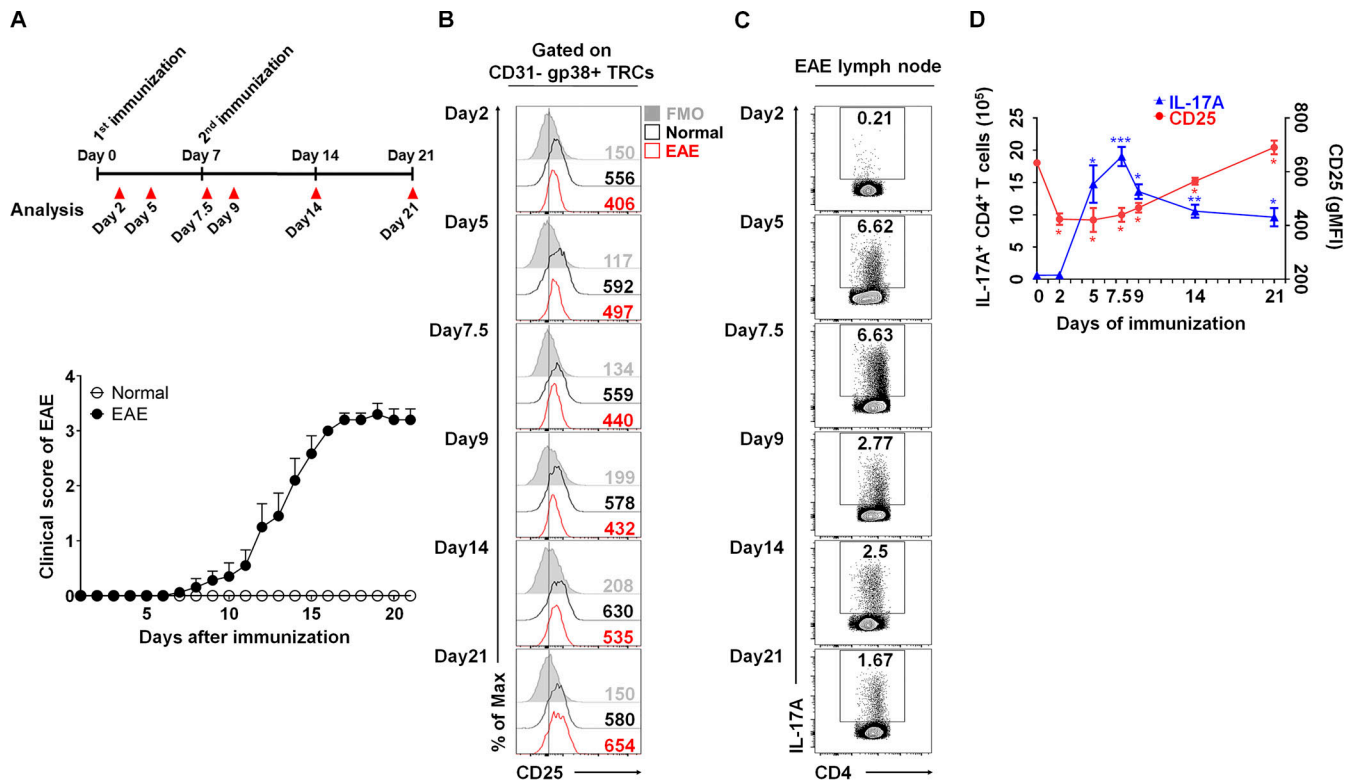
Figure 4. **Dynamic expression of CD25 on TRCs during EAE induction. (A)** The overall scheme and severity of EAE induction ($n \geq 10$ per each group). **(B)** The expression of CD25 on CD31⁻gp38⁺ gated TRC population from normal (black lines) or EAE-induced (red lines) freshly isolated iLNs is shown by flow cytometric histograms at the designated time points. Gray histograms represent isotype control. **(C)** The frequency of IL-17A–producing CD4⁺ T cells in iLN, as detected by flow cytometry at the indicated time points. **(D)** Compiled data show the kinetics of IL-17A⁺CD4⁺ T cells and CD25⁺ TRCs in iLN during EAE induction. *, $P < 0.05$; **, $P < 0.01$; ***, $P < 0.001$ compared with day 0 results. Error bars indicate the mean ± SEM ($n = 4$ per each group). Data are representative of three independent experiments.

recipients (Fig. S4 B). To evaluate the in vivo differentiation of CD4⁺ T cells, we quantified the frequency of Th1 and Th17 cells. CD25⁻/⁻RAG-1⁻/⁻ recipients showed increased numbers of IL-17A–producing CD4⁺ T cells in both the central nervous system (CNS) and iLNs (Fig. S4, C and D). Thus, these results indicate that CD25 deficiency aggravates the severity of EAE through augmentation of in vivo Th17 cell differentiation.

A recent study revealed CD25 expressing DCs *trans*-present IL-2 for DC-mediated T cell activation (Wuest et al., 2011). Because CD25 is also absent on DCs of CD25⁻/⁻RAG-1⁻/⁻ recipients, diminished Th17 cell differentiation due to reduced IL-2 responses by CD4⁺ T cells could be a result of defunctionalization of IL-2 *trans*-presenting DCs. Therefore, to exclude this possibility, we generated a bone marrow transplantation (BMT) model in which BM-derived from CD45.1 WT (donor) mice was injected i.v. into irradiated CD45.2 WT or CD45.2 CD25⁻/⁻ (recipient) mice (Fig. 5 A). Cells were gated to enumerate T cells originating from donor BM (Fig. 5 B). More than 90% of peripheral cells were found to be reconstituted from donor-derived BM cells 8 wk after BMT (Fig. 5 C). Moreover, CD25-deficient mice reconstituted with CD25-expressing DCs (BMT^WT→CD25–/–) exhibited significantly increased EAE symptoms compared with WT-reconstituted recipients (BMT^WT→WT; Fig. 5 D), and the onset of EAE in BMT^WT→WT mice was delayed compared with that of BMT^WT→CD25–/– mice (Fig. 5 E). In

addition, CD4⁺ T cells in the CNS and iLNs in BMT^WT→CD25–/– mice showed more IL-17A–producing capacity than those from BMT^WT→WT mice (Fig. 5, F and G), which suggests that CD25 deficiency in nonhematopoietic cells, such as LN-TRCs, causes elevated Th17 cell differentiation. Finally, splenic CD4⁺ T cells from both mice were restimulated with MOG_{35–55} peptides to determine recall responses after in vivo immunization. Splenic CD4⁺ T cells from the BMT^WT→CD25–/– mice secreted higher amounts of IL-17A than did those from BMT^WT→WT mice, whereas IFN-γ production was reduced (Fig. 5 H). Therefore, these results suggest that CD25 deficiency in stromal cells, such as LN-TRCs, results in enhanced Th17 differentiation and exacerbation of EAE phenotypes.

LN-TRC–specific CD25 deficiency exacerbates Th17 cell–mediated experimental autoimmunity

To further confirm the enhanced Th17 responses induced by CD25-deficient LN-TRCs, we generated LN-TRC–specific CD25-deficient (CD25^fl/flCCL19^cre) mice by crossing CD25^fl/fl mice, which were generated by crossing with flippase knock-in mice (Fig. S5 A), with CCL19^cre mice. As expected, we observed that CD25 expression is deleted only on LN-TRCs (Fig. S5 B, upper panel), and its expression remains intact on other immune cells including CD4⁺ T cells, CD8⁺ T cells, CD11c⁺ DCs, and B220⁺ B cells from CD25^fl/flCCL19^cre mice (Fig. S5 B, lower panel). After
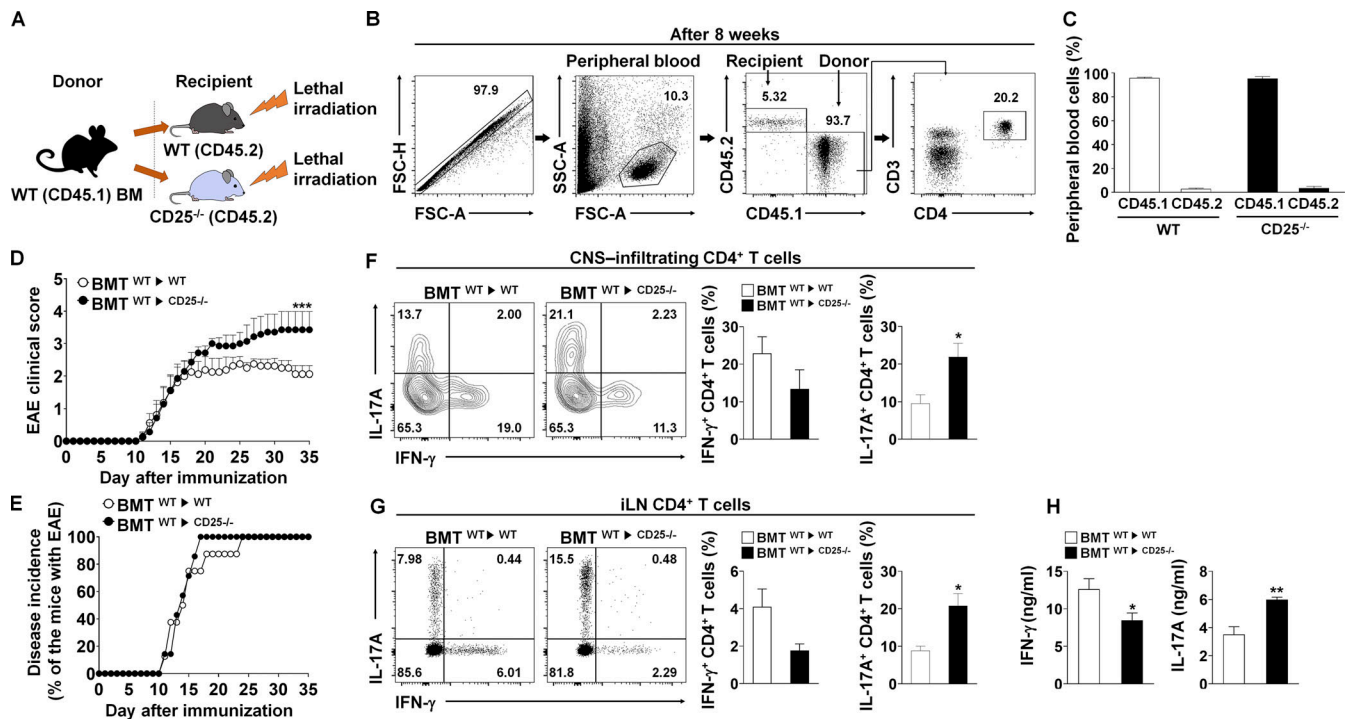
Figure 5. **The severity of EAE is exacerbated in BM cell–transplanted CD25-deficient mice. (A)** Schematic showing design of the experimental BMT model. **(B)** Gating strategy for FACS analysis of peripheral blood cell populations in reconstituted mice 8 wk after lethal irradiation (900 rad) and BM cell (5 × 10^6) transplantation. Cells were first gated for singlets (forward scatter height vs. area [FSC-H vs. FSC-A]) and lymphocytes (side scatter area [SSC-A] vs. FSC-A). The lymphocyte populations were further analyzed for the expression of CD45.1 and CD45.2 markers. CD3 or CD4 surface expression was then determined in this gated population. **(C)** Quantification of CD45.1$^+$ and CD45.2$^+$ cells after BMT ($n \geq 8$ per each group). **(D)** BM cells were transplanted into either WT (BM$^{WT \to WT}$, $n = 8$) or CD25$^{-/-}$ (BM$^{WT \to CD25-/-}$, $n = 7$) recipient mice, and EAE was induced. Clinical scores of EAE representing disease severity are depicted. *, P < 0.05 compared with EAE-induced BM cell–transplanted WT mice. Error bars indicate the mean ± SEM. **(E)** Disease incidence in WT (BM$^{WT \to WT}$) and CD25$^{-/-}$ (BM$^{WT \to CD25-/-}$) mice was measured for the indicated length of time after immunization. **(F and G)** Intracellular production of IFN-γ and IL-17A from CD4$^+$ T cells in the CNS (F) or iLNs (G) of EAE-induced mice. Representative flow cytometric plots (left) and compiling data (right) are depicted. *, P < 0.05 compared with EAE-induced BM cell–transplanted WT mice. Error bars indicate the mean ± SEM. **(H)** The levels of cytokine production were measured by ELISA in culture supernatants from antibody-restimulated splenocytes. *, P < 0.05; **, P < 0.01 compared with the EAE-induced BM cell–transplanted WT mice. Error bars indicate the mean ± SEM. Data are representative of three independent experiments.

immunization of WT littermates or CCL19^{cre} and LN-TRC–specific CD25-deficient CD25$^{fl/fl}$CCL19^{cre} mice with MOG$_{35-55}$ peptides, we analyzed the phenotypes of EAE. As shown in Fig. 6 A, CD25$^{fl/fl}$CCL19^{cre} mice developed more severe EAE symptoms compared with CCL19^{cre} mice. Furthermore, CCL19^{cre} control mice showed a slightly delayed onset of EAE, although there was no significant difference in disease incidence (Fig. 6 B). Consistent with the in vivo results, CD25$^{fl/fl}$CCL19^{cre} mice contained more IL-17A–producing CD4$^+$ T cells in the CNS, iLN, and spleen, whereas IFN-γ–producing cell numbers were reduced compared with those of CCL19^{cre} mice (Fig. 6, C–E). We further examined IFN-γ, IL-4, and IL-17A cytokine levels in T cells of these mice, and found that production of IL-17A by CD4$^+$ T cells from CD25$^{fl/fl}$CCL19^{cre} mice was elevated over that of CCL19^{cre} mice, whereas IFN-γ and IL-4 production were reduced (Fig. S5 C). Because it is well known that IL-2 signaling not only induces T cell activation, but also plays an important role in the development of Foxp3$^+$ regulatory T (Treg) cells (Setoguchi et al., 2005), we quantified CD25$^+$Foxp3$^+$CD4$^+$ Treg cells in the iLNs and spleens of these mice. However, no significant differences were detected in the induction of Treg cells by CCL19^{cre} and CD25$^{fl/fl}$CCL19^{cre} mice (Fig. S5 D). Collectively, these results

suggest that LN-TRC–specific CD25 deletion enhances Th17 cell differentiation and, consequently, CNS accumulation in vivo, leading to more severe EAE.

The endothelial blood–brain barrier in CNS also produces CCL19 and regulates lymphocyte recruitment during EAE (Alt et al., 2002), and the incidence of EAE may be affected by CCL19 producing blood–brain barrier endothelium in our conditional knockout mouse model. Thus, to further confirm the role of CD25 on TRCs in Th17 cell differentiation, we assessed two other Th17-related autoimmune disease models, experimental psoriasis and AIA, in CD25$^{fl/fl}$CCL19^{cre} mice. As shown in Fig. 7, after imiquimod (IMQ) treatment, a gross skin examination of CD25$^{fl/fl}$CCL19^{cre} mice revealed aggravated psoriatic manifestation with enhanced erythema, epidermal thickening, and skin scaling compared with that of CD25$^{fl/fl}$ mice (Fig. 7, A and C). H&E staining of dorsal skin from CD25$^{fl/fl}$CCL19^{cre} mice revealed increased epidermal thickness and parakeratosis (Fig. 7 B). IL-17A$^+$ CD4$^+$ T cell populations in iLNs were significantly higher in CD25$^{fl/fl}$CCL19^{cre} mice than in CCL19^{cre} mice (Fig. 7 D). Finally, AIA as a model for Th17-mediated inflammatory arthritis was also studied to investigate the effects of CD25 in TRCs on in vivo Th17 differentiation (Bush et al., 2002; Sarkar et al., 2010). The
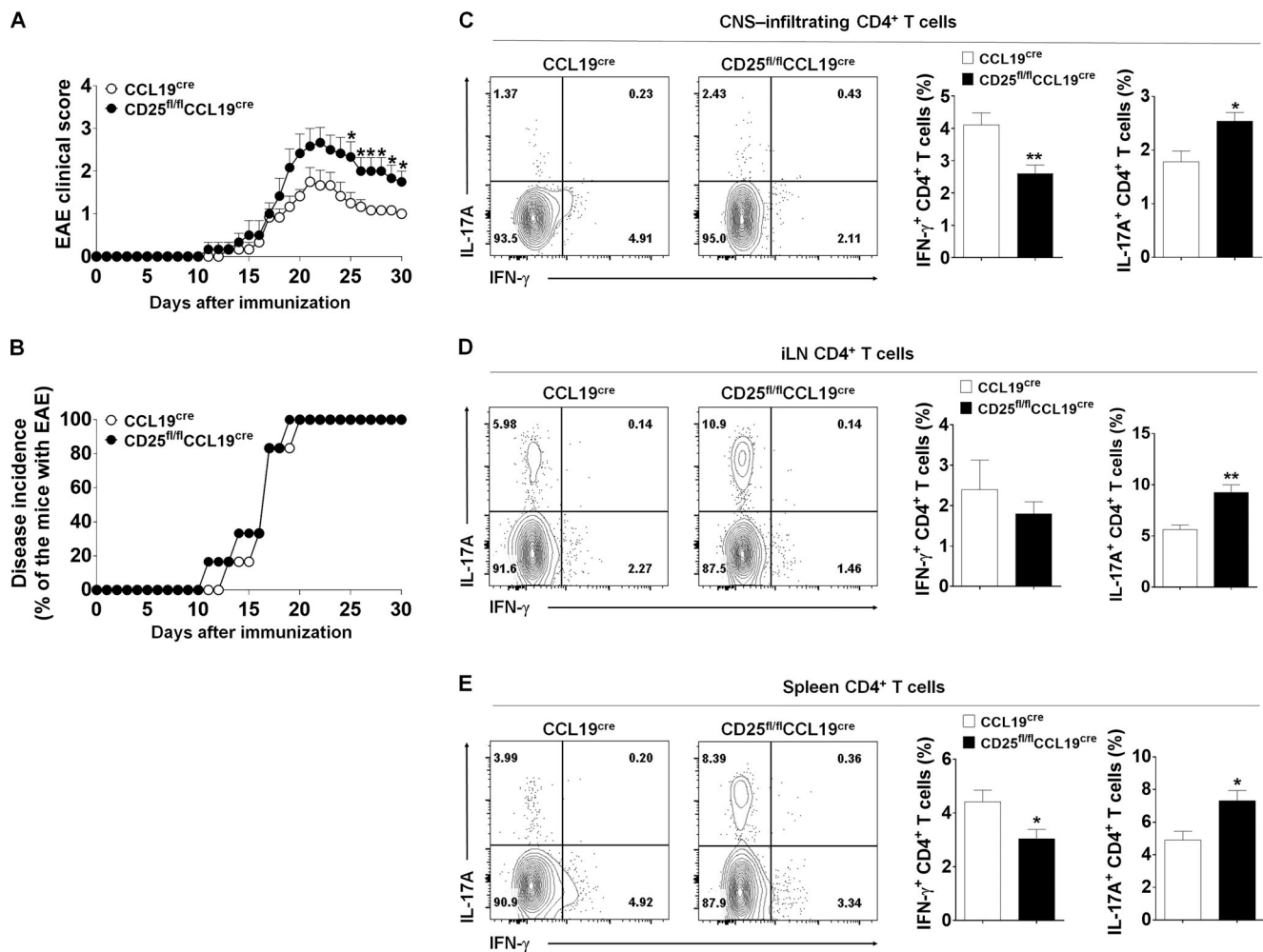
Figure 6. CD25$^{fl/fl}$CCL19^{cre} mice exhibit more severe EAE and higher Th17 cell differentiation vs. controls. (A) EAE was induced in CCL19^{cre} and CD25$^{fl/fl}$CCL19^{cre} mice, and disease severity was measured. *, P < 0.05; ***, P < 0.001 compared with EAE-induced CCL19^{cre} mice (n = 6 per each group). **(B)** EAE incidence was assessed for the indicated length of time. **(C–E)** Inflammatory cells were extracted from CNS-infiltrating (C), iLNs (D), and spleens (E) of EAE-induced mice and analyzed for cytokine production. *, P < 0.05; **, P < 0.01 compared with the EAE-induced CCL19^{cre} mice. Error bars indicate the mean ± SEM. Data are representative of three independent experiments.

arthritic severity of AIA, including joint inflammation, cartilage destruction, and IL-17A-producing CD4$^+$ T cells in iLNs was more pronounced in CD25$^{fl/fl}$CCL19^{cre} compared with CCL19^{cre} mice (Fig. 7, E–G), suggesting that the CD25 deficiency on LN-TRCs affects Th17-associated autoimmune and inflammatory disorders.

The amount of IL-2 loaded by LN-TRCs is decreased by CD25 deficiency

Finally, to further understand the underlying mechanism of the CD4$^+$ T cell–IL-2–CD25 axis on TRCs, we quantified bound IL-2 and CD4$^+$ T cells on the surface of TRCs. For this, we first visualized the amount of IL-2 and CD4$^+$ T cells loaded by CD25 on TRCs using confocal microscopy. Purified naive CD4$^+$ T cells from dsRed mice expressing RFP were loaded on either WT or CD25-deficient TRCs in the presence of exogenous IL-2 for 1 h. After light wash, IL-2 and gp38 were labeled with fluorescently tagged antibodies to visualize the TRC–IL-2–CD4$^+$ T cell complex. We detected a significantly lower number of RFP-expressing

CD4$^+$ T cells and less IL-2 on CD25-deficient TRCs (Fig. 8 A), which was confirmed by quantification analysis (Fig. 8 B). To further demonstrate CD25-mediated IL-2 *trans*-presentation by TRCs, we performed a proximity ligation assay (PLA) in which fluorescence is observed only after two antibodies against CD25 and IL-2 interact each other. After incubation, we detected fluorescence only in CD25-expressing WT TRCs, and the fluorescence intensity was further enhanced after addition of rIL-2 (Fig. 8 C). On the contrary, fluorescence intensity was hardly detected on CD25-deficient TRCs regardless of rIL-2 addition. Thus, the colocalization of IL-2 and CD4$^+$ T cells was significantly reduced in the presence of CD25-deficient TRCs. These results suggest that LN-TRCs load IL-2 onto CD25 during cell–cell contact between CD4$^+$ T cells and LN-TRCs (Fig. 8 D).

Discussion

In this study, we demonstrate for the first time that LN-TRCs regulate differentiation of naive CD4$^+$ T cells by modulating IL-2
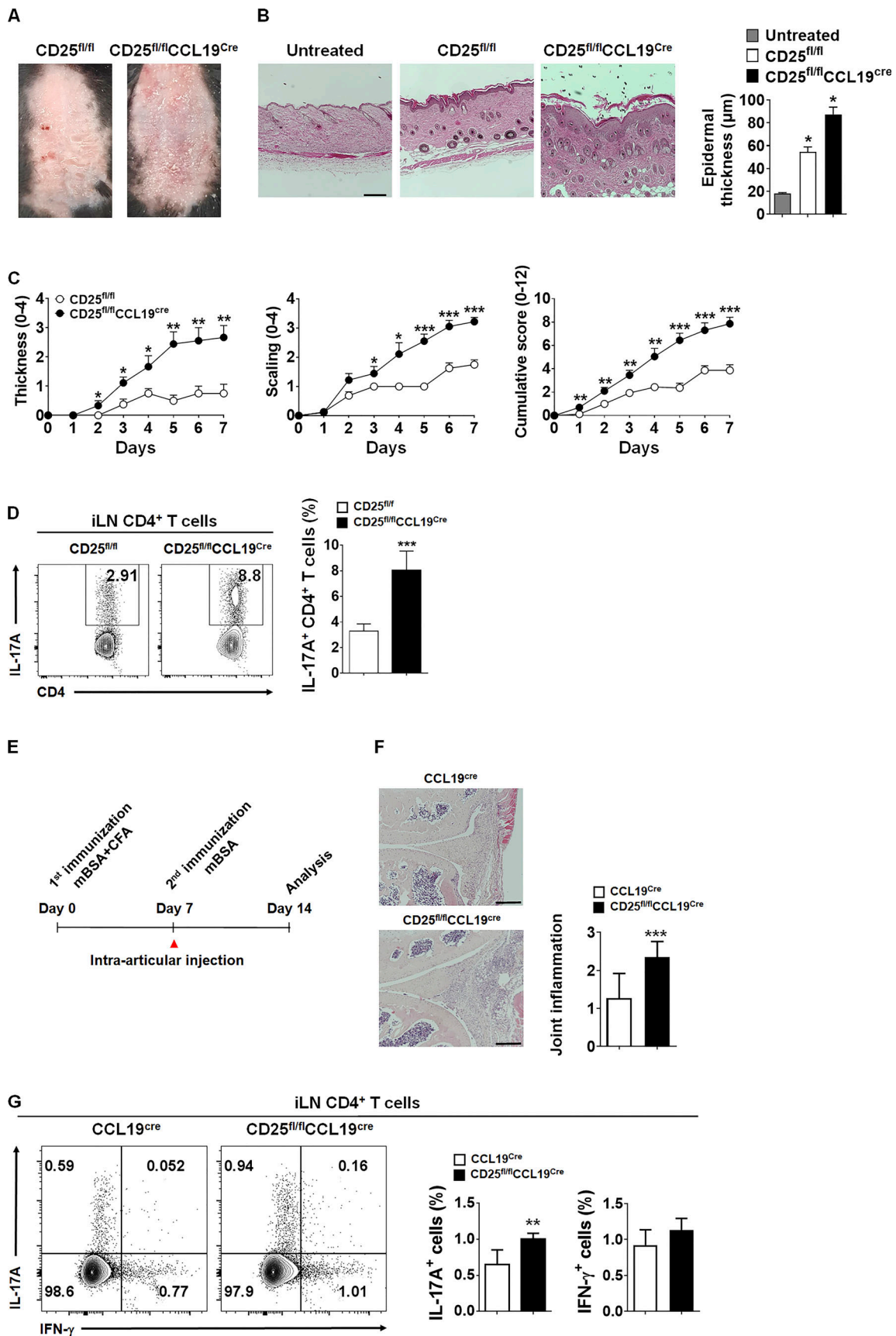
Figure 7. **Experimental psoriasis and AIA are aggravated in mice with TRC-specific CD25 deletion. (A)** Representative image of phenotypical psoriasiform skin lesions from IMQ-treated CD25^{fl/fl} and CD25^{fl/fl}CCL19[cre] mice. **(B)** H&E-stained skin sections and compiled data of epidermal thickness are depicted. Scale

bar = 250 µm. *, P < 0.05 compared with CD25^{fl/fl} mice. Error bars indicate the mean ± SEM (n = 8 per each group). **(C)** The severity of thickness and scaling on back skin and cumulative scores were evaluated in IMQ-treated CCL19[cre] and CD25^{fl/fl}CCL19[cre] mice. The cumulative score of psoriasis area and severity index includes skin thickness, scaling, and erythema scores. *, P < 0.05; **, P < 0.01; ***, P < 0.001 compared with CD25^{fl/fl} mice. Error bars indicate the mean ± SEM (n = 8 per each group). **(D)** IL-17A^{+} CD4^{+} T cell populations were analyzed by flow cytometry. Representative flow cytometric plots (left) and compiled data (right) are described. ***, P < 0.001 compared with CD25^{fl/fl} mice. Error bars indicate the mean ± SEM (n = 8 per each group). **(E)** The experimental scheme of AIA model. CCL19[cre] and CD25^{fl/fl}CCL19[cre] mice were immunized with mBSA emulsified with CFA as described in Materials and methods. **(F)** Pathological sections of CCL19[cre] and CD25^{fl/fl}CCL19[cre] mouse knee joints stained with H&E (left). Scale bar = 250 µm. Compiling data are depicted (right). ***, P < 0.001 compared with CCL19[cre] mice. Error bars indicate the mean ± SEM (n = 5–6 per each group). **(G)** IFN-γ^{+} and IL-17A^{+} CD4^{+} T cell populations after mBSA restimulation were analyzed by flow cytometry from iLNs of AIA-induced mice. Flow cytometry (left) and compiling data (right) are described. **, P < 0.01 compared with CCL19[cre] mice. Error bars indicate the mean ± SEM (n = 5–6 per each group). Data are representative of three independent experiments.

signaling. We provide evidence that LN-TRCs express the CD25 subunit of IL-2R, which plays an important role in *trans*-presentation of IL-2 to neighboring CD4^{+} T cells to facilitate early IL-2–mediated signaling. Further, CD25 deficiency in LN-TRCs enhances the phenotypes of autoimmune diseases through increased differentiation of Th17 cells. Thus, our study suggests that CD25 on LN-TRCs is an immune modulator that plays a crucial role in the inflammatory autoimmune responses by *trans*-presenting IL-2 to neighboring CD4^{+} T cells.

The role of LNSCs in T cell homeostasis and of their cross talk with hematopoietic cells for the regulation of immune cell function have been studied previously (Mueller and Germain, 2009). Moreover, Link et al. (2007) reported that CD4^{+} T cells cocultured with LN-TRCs significantly enhance cell survival compared with CD4^{+} T cells cultured alone. Furthermore, although we found that the viability of CD4^{+} T cells increased upon stimulation with anti-CD3 and CD28 antibodies, coculture with TRCs further increased T cell viability more than that induced
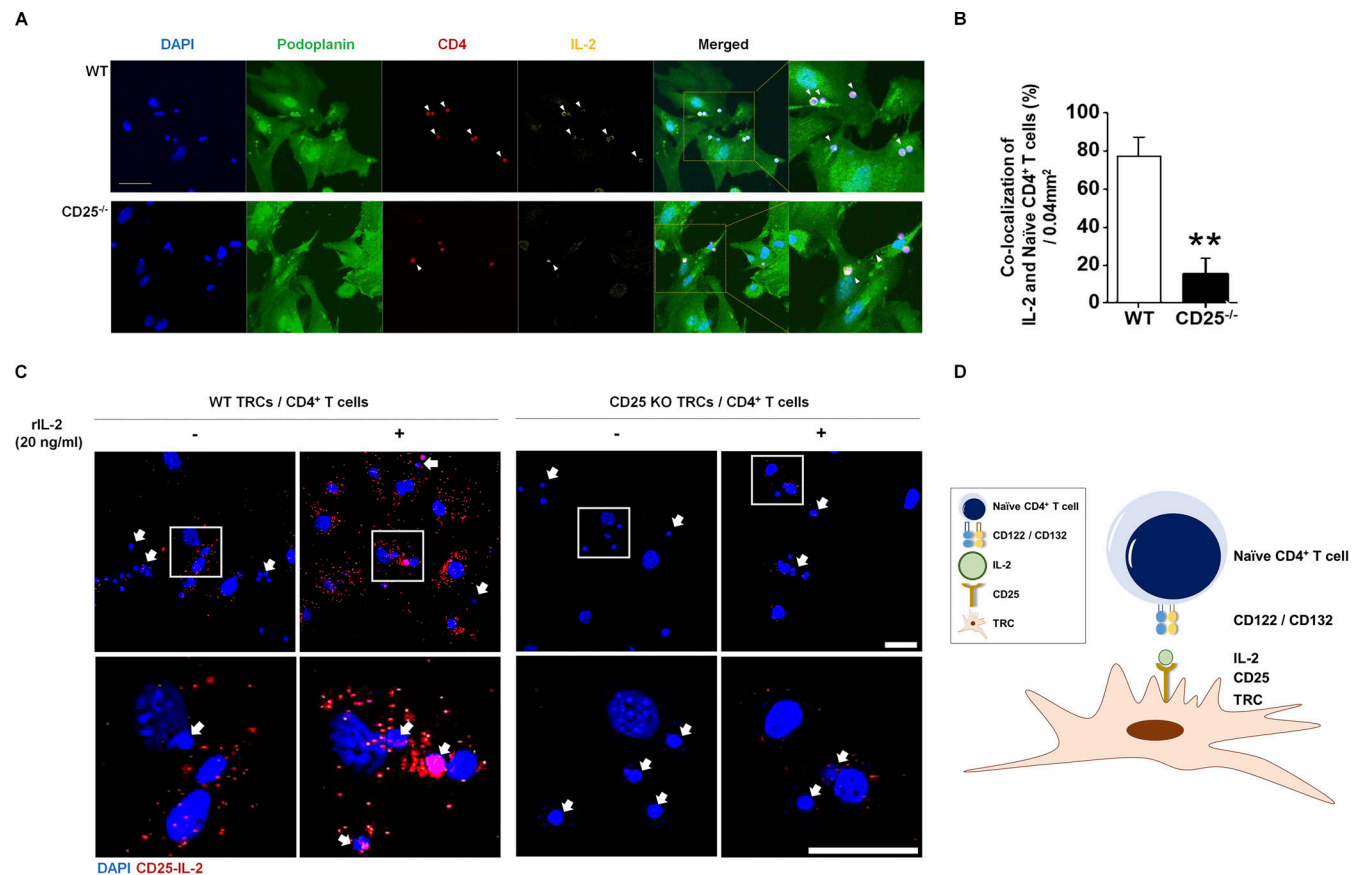

Figure 8. Colocalization of IL-2 and CD4^{+} T cells on TRCs and complex of IL-2 and CD25. Purified, naive CD4 T cells (1 × 10^{6}) from dsRed mice were cocultured with WT or CD25-deficient TRCs (1 × 10^{5}). rIL-2 (20 ng/ml) was treated to each well. **(A)** After 1-h incubation and light wash, images were visualized by confocal microscopy. Arrowheads indicate colocalization of rIL-2 and CD4^{+} T cell on TRCs. Immunofluorescence staining of nuclear DAPI (blue), podoplanin (green) for TRCs, RFP-expressing CD4^{+} T cells isolated from dsRed mice (red), and rIL-2 (yellow). Scale bar = 50 µm. **(B)** Quantification of rIL-2 and colocalized CD4^{+} T cells are depicted. **, P < 0.01 compared with WT. Error bars indicate the mean ± SEM (n = 4 per each group). **(C)** Purified, naive CD4 T cells (1 × 10^{5}) were cocultured with WT or CD25-deficient TRCs (2 × 10^{4}). rIL-2 (20 ng/ml) was added to each well. After 1-h incubation, IL-2–CD25 complexes on TRC were visualized by PLA. Nuclear DAPI staining (blue); CD25-IL-2 complex (red). Arrows indicate CD4^{+} T cells. Scale bar = 50 µm. **(D)** TRCs form immune synapses with CD4^{+} T cells through their CD25 complexed with IL-2. Data are representative of three independent experiments.

by antibody stimulation. TRCs likely play more important roles, such as providing IL-7 and CCL19/21 for T cell homeostasis, than in vitro stimulation for CD4⁺ T cell survival. TRCs have been previously studied for their effects on the viability of naive CD4⁺ T cells; however, their roles in proliferation and differentiation of naive CD4⁺ T cells are almost unknown. To this end, we show that coculture with TRCs results in significantly enhanced proliferation and differentiation of CD4⁺ T cells relative to T cell culture alone after anti-CD3 and CD28 antibody stimulation. Therefore, we propose that LN-TRCs are essential for the enhanced biological activity of CD4⁺ T cells.

Of IL-2R components, CD25 is the only one specifically expressed on LN-TRCs. Thus, we speculate that CD25 expression on TRCs, which is responsible for communication with neighboring CD4⁺ T cells, is associated with immune responses in LN microenvironments. Because naive CD4⁺ T cells migrate along the TRC network into the T cell zones of the LN paracortex, TRCs come in close contact with T cells to form a synapse with naive CD4⁺ T cells, similar to the DC–T immunological synapse. Although CD25 binds to IL-2 with lower affinity than the CD122 and CD132 complex does (Wang et al., 2005), a previous study reported that IL-2 *trans*-presentation occurs when IL-2 exists in the small confines of an immune synapse (Chirifu et al., 2007). Thus, we hypothesized that CD25 on LN-TRCs binds to IL-2 in a synaptic cleft, leading to early IL-2 *trans*-presentation to neighboring naive CD4⁺ T cells during T cell activation. It should be noted that DCs also use the TRC network to traffic within the T cell zones of LNs. This occurs through an interaction between DC-expressed CLEC-2 and gp38 expressed on LN-TRCs (Acton et al., 2012). Although CD25 on DCs promotes early high-affinity IL-2 signaling with the IL-2R on T cells through *trans*-presentation (Wuest et al., 2011), our assumption is that naive CD4⁺ T cells may first interact with TRCs rather than DCs and then react with IL-2, which might exist in small amounts in the LNs. Thus, IL-2 is first influenced by CD25 on LN-TRCs before being *trans*-presented by CD25 on DCs. The IL-2–CD25 complex binds to IL-2Rβ with much higher affinity than does IL-2 alone, and the reactivity of IL-2 on IL-2R is stronger in the presence of CD25 (Wang et al., 2005). In the present study, we observed that STAT5 phosphorylation in naive CD4⁺ T cells was significantly enhanced by the addition of exogenous rIL-2 when naive CD4⁺ T cells were cocultured with WT TRCs compared with coculture with CD25-deficient TRCs. This suggests that CD25 expression on LN-TRCs influences IL-2 responsiveness of naive CD4⁺ T cells, likely through transfer of IL-2 by CD25 to neighboring cells in a *trans* manner. Hence, CD25 expression on LN-TRCs regulates differentiation of naive CD4⁺ T cells into Th cell lineages, including Th1, Th2, and Th17. Furthermore, we show here that the coculture of naive CD4⁺ T cells with CD25-deficient LN-TRCs results in increased Th17 cell differentiation. This suggests that deficiency or reduction of CD25 on LN-TRCs might be related to Th17-associated autoimmune and inflammatory diseases. B cells, T cells, and DCs are well-known producers of IL-2 in peripheral tissues (Boyman and Sprent, 2012), and IL-2 derived from DCs is one of key cytokines for T cell activation and proliferation (Granucci et al., 2001; Owen et al., 2018). So, we highly consider both T cells and DCs as major sources for IL-2 in

our model, even though we did not show actual IL-2 production by DCs.

The pathogenic roles of Th17 cells in autoimmune diseases such as MS, psoriasis, and RA have been well described (Tesmer et al., 2008). Therefore, we first examined the kinetics of CD25 expression on TRCs during EAE induction. Immediately after immunization, the expression of CD25 on TRCs decreased and at later time points the Th17 cell population dramatically increased. The down-regulation of CD25 on TRCs occurred before EAE onset, suggesting the possibility that CD25 dynamics on LN-TRCs at early time points controls the differentiation of naive CD4⁺ T cells. To further clarify the effects of CD25 expressed on LN-TRCs on Th17 cell differentiation in vivo, we generated various EAE mouse models. Using these models, we show that CD25-deficient CD45.2 recipient mice (BMT^WT→CD25−/−), injected with BM derived from WT CD45.1, also develop more severe EAE and accumulate more Th17 cells in the CNS than BM reconstituted WT CD45.2 recipient mice (BMT^WT→WT). Furthermore, adoptive-transfer experiments revealed increased severity of EAE in MOG-immunized CD25−/−RAG1−/− recipients adoptively transferred with naive CD4⁺ T cells compared with MOG-immunized RAG1−/− recipients. The clinical features of EAE in adoptive-transfer mice were more severe than those in BMT-recipient mice, likely because of more efficient IL-2 signaling in CD4⁺ T cells mediated by other factors, such as secreted IL-2 and CD25-mediated *trans*-presentation of IL-2 by DCs during T cell activation in RAG1−/− mice.

Finally, we generated TRC-specific CD25-deficient (CD25^fl/fl^CCL19^cre) mice and verified the roles of CD25 on TRCs in Th17 cell–related autoimmune diseases including MS, psoriasis, and RA (Volin and Shahrara, 2011). Of particular interest, TRC-specific CD25 deletion exacerbates the severity of autoimmune diseases, including EAE, psoriasis, and AIA, and increases induction of IL-17A–producing CD4⁺ T cells in mice. Thus, the ability to inhibit autoimmune diseases mediated by Th17 cells is dependent on LN-TRCs that can present IL-2 to CD4⁺ T cells in a *trans* manner. We showed that CD25-expressing LN-TRCs regulate CD4⁺ T cell differentiation via modulating IL-2–mediated signaling. However, we cannot rule out that other SCs such as LECs in LNs participate in regulating CD4⁺ T cell differentiation and tolerance via CD25 expression. These possibilities are supported by the results that the EAE phenotypes in BM chimeric mice seemed to be stronger than those of LN-TRC–specific CD25-deficient mice. Additionally, although we clearly showed that the initial in vitro proliferative capacity of naive CD4⁺ T cells is similar cocultured with WT or CD25-deficient TRCs, our in vivo data have not directly demonstrated an influence of TRC CD25 on priming on the T cell proliferative responses in the LNs or spleen.

Interestingly, several studies have demonstrated that peripheral tolerance can be mediated by at least three different LNSC populations including extrathymic Aire expressing cells, TRCs, and LECs (Cohen et al., 2010; Fletcher et al., 2010a; Gardner et al., 2008; Saxena et al., 2019). Through the expression of peripheral tissue–specific antigens, Aire-expressing extrathymic SCs can induce the deletion of self-reactive CD8⁺ T cells. Similarly, peripheral tissue–restricted antigen-

Kim et al.
LN-TRC–mediated T cell regulation

Journal of Experimental Medicine
https://doi.org/10.1084/jem.20200795

11 of 16

expressing LN-TRCs can directly mediate tolerization of CD8+ T cells. In the case of LECs, they can induce peripheral tolerance by direct presentation of self-antigens to CD8+ T cells, which is dependent on PD-L1 expression. Furthermore, it has been shown that LNSCs such as TRCs and LECs mediated nitric oxide production controls expansion of the recently activated T cell pool in LNs (Lukacs-Kornek et al., 2011). Although many studies demonstrate peripheral tolerance by these SCs, immune stimulation is also suggested especially in the case of inflammatory conditions.

In addition, we visualized the colocation of CD4+ T cells and IL-2 complex formation on TRCs and proximal ligation of CD25 and IL-2 only on WT TRCs. Our data showed that exogenous IL-2 can form a complex with LN-TRC membrane–expressed CD25, presented *in trans* to naive CD4+ T cells. TRCs lacking CD25 failed to colocalize to IL-2 and naive CD4+ T cells, suggesting that TRCs present IL-2 in a *trans* manner to naive CD4+ T cells in T cell zones of LNs through CD25; thus, IL-2 signaling is likely induced during the formation of the immunological synapse with CD4+ T cells through IL-2 *trans*-signaling.

Several studies have reported the infiltration of IL-17–expressing CD4+ T cells into the synovium (Yoo et al., 2019) and synovial fibroblast activation by IL-17 and TNF-α (Parsonage et al., 2008), suggesting that fibroblast-like synoviocytes (FLSs) might have a role similar to that of LN-TRCs in the rheumatoid synovial microenvironment. Further studies using gene expression profiling will be required to understand whether FLSs express CD25 and if colocalization of IL-2 and CD25 on FLS regulates CD4+ T cell function in RA patients. It will also be interesting to investigate the expression of CD25 by other fibroblasts and dynamic expression of CD25 on the fibroblasts during the progression of autoimmunity.

In summary, our findings provide evidence that the dynamic expression of CD25 on TRCs, such as stress-induced reduction or acute/chronic inflammation-mediated down-regulation, might increase Th17 cell differentiation and enhance the incidence of Th17-associated autoimmune diseases. Therefore, CD25 expression levels on LN-TRCs and IL-2 *trans*-signaling might be good biomarkers for assessing predisposition to autoimmune diseases.

Materials and methods

Mice
C57BL/6-CD45.1 (JAX:002014), C57BL/6, Rag-1−/− (JAX:002216), CD25−/− (JAX:002462), and FLPe (JAX:003946) mice were purchased from Jackson Laboratories. Il2ra$^{tm1a(EUCOMM)Wtsi}$ (EM:08466) and CCL19^{cre} (EM:09381) mice were purchased from EMMA (Chai et al., 2013). CD25−/−RAG1−/− and CD25$^{fl/fl}$CCL19^{cre} were bred in-house in our specific pathogen–free animal facility. Il2ra$^{tm1a(EUCOMM)Wtsi}$ mice were crossed with FLPe mice to generate CD25-floxed (CD25$^{fl/fl}$) mice. These mice were crossed with CCL19^{cre} to specifically delete CD25 expression in TRCs. Age-matched (8–9 wk old) mice were used in all experiments, and littermates were as controls. Animal care and experimental procedures were performed with the approval of the Animal Care Committee of Korea Advanced Institute of Science and Technology (KA2013-32).

CD4+ T cell isolation
Naive CD4+ T cells from the spleens of WT C57BL/6 mice were purified with the Mouse CD4 Naive T cell Enrichment Kit according to the manufacturer's (eBioscience) instructions (purity >95%).

Stromal cell isolation and TRC purification
LNs were isolated from WT or CD25-deficient mice. LNs were digested in 5 ml of an enzyme mix containing 0.2 mg/ml type II collagenase (Worthington), 0.1 mg/ml DNase I (Roche), and 0.8 mg/ml Dispase (Gibco) at 37°C with shaking for 30 min. At 10-min intervals, digested LNs were pipetted. The digested LNSC suspension was filtered through a 40-μm nylon cell strainer and cultured in 100-mm dishes in DMEM (Thermo Fisher Scientific) supplemented with 10% FBS (Thermo Fisher Scientific) and 1% penicillin-streptomycin (Gibco). The next day, the medium was changed to remove suspension cells, and the remaining stromal cells were allowed to grow for 5 d before cells were stained with indicated antibodies. CD45−CD31−gp38+ TRCs were sorted using a FACS Aria II (BD Biosciences). TRCs used in experiments were >95% pure.

Coculture of CD4+ T cells with TRCs
Isolated and purified TRCs were cultured in a 24-well plate (2 × 10⁴/well). After overnight adhesion, 2 × 10⁵ naive CD4+ T cells and irradiated (3,000 rad) APCs along with anti-CD3 (BD Biosciences) and anti-CD28 (BD Biosciences) monoclonal antibodies (3 and 1 μg/ml each) were added and cultured for 3 days in RPMI-1640 supplemented with 10% FBS and 1% penicillin-streptomycin at 37°C in a humidified 5% CO_2 atmosphere.

Cell proliferation assay
Purified naive CD4+ T cells were labeled with CFSE (Invitrogen) for 5 min. CFSE-labeled T cells, irradiated APCs, and anti-CD3 and anti-CD28 antibodies were added to plates with or without TRCs. CFSE dilution was analyzed by flow cytometry after 3–4 d of culture.

Adoptive transfer of naive CD4+ T cells
Naive CD4+ T cells (5 × 10⁶) from CD45.1 C57BL/6 WT mice were administered (100 μl, i.v.) via adoptive transfer into RAG-1−/− or CD25−/−RAG-1−/− mice.

BMT
WT and CD25−/− mice (8–9 wk old) were lethally irradiated with a total dose of 900 rad (X-RAD 320; Precision X-ray) in a split dose separated by 6 h. Mice were reconstituted intravenously with WT CD45.1 BM cells (5 × 10⁶) from tibias and femur bone cavities. After 8 wk, BM-transplanted chimeric mice were confirmed by flow cytometric analysis. Using this protocol, we produced two types of BM-transplanted mice: WT BM cells to WT mice (BMT$^{WT→WT}$) and WT BM cells to CD25-deficient mice (BMT$^{WT→CD25−/−}$).

Western blot analysis
Cells were lysed in radioimmunoprecipitation assay buffer (50 mM Tris, pH 7.5, 150 mM NaCl, 1% NP-40, and 1 mM EDTA)

Kim et al.
LN-TRC–mediated T cell regulation

Journal of Experimental Medicine
https://doi.org/10.1084/jem.20200795

12 of 16

containing phosphatase inhibitor cocktail (Roche) and protease inhibitor cocktail (Roche), incubated on ice for 30 min, and collected by centrifugation at 13,000 rpm for 10 min. For immunoblotting, membranes were incubated with the T-bet (1:1,000; Thermo Fisher Scientific), GATA3 (1:1,000; BD Biosciences), and RORγt (1:1,000; BD Biosciences) primary antibody overnight at 4°C, followed by incubation with 1:4,000 dilution of HRP-linked secondary antibody for 1 h at room temperature. β-Actin was probed with the corresponding antibody to assure equal loading. Finally, immunoreactive proteins were detected using the enhanced chemiluminescence assay with HRP (Thermo Fisher Scientific).

Cytokine ELISA
Cytokine detection in the culture supernatant was performed in triplicate by sandwich ELISA as previously described (Kim et al., 2017a). Briefly, 96-well plates (Greiner) were precoated with 40 µl of 1:500 diluted capture antibody and incubated for 2 h at 37°C. Next, plates were washed and blocked with 200 µl of 0.2% I-block (Applied Biosystems) overnight at 4°C. After washing, 40 µl of the collected supernatant samples were transferred to the plates. The washes were repeated, and 40 µl of 1:500 detection antibody was added and incubated for 2 h at 37°C. After another wash, 40 µl of streptavidin-alkaline phosphatase (BD Biosciences) diluted in PBS/Tween/BSA (1:1,000 dilution) was added, and the plates were incubated at room temperature for 30 min. After the final wash, 70 µl of alkaline phosphatase substrate (5 mmol/l of p-nitrophenyl phosphate substrate in 0.1 mol/l alkaline buffer; Sigma-Aldrich) was added and incubated for color development at room temperature. When color development was sufficient, the reaction was terminated by adding 40 µl of 0.5 N sodium hydroxide. Optical density was measured at 405 nm using an ELISA plate reader (Thermo Fisher Scientific). Anti-mouse-IFN-γ, IL-4, and IL-17A antibodies were prepared for use as capture antibodies (IFN-γ and IL-4 from BD Biosciences, IL-17A from Thermo Fisher Scientific). Biotin-conjugated detection antibodies against IFN-γ, IL-4, and IL-17A were used (IL-4 from BD Biosciences, IFN-γ and IL-17A from Thermo Fisher Scientific). Recombinant IFN-γ (Thermo Fisher Scientific), IL-4 (BD Biosciences), and IL-17A (Peprotech) were used as ELISA standards.

Intracellular cytokine staining (ICS)
Single-cell suspensions prepared from CNS, iLNs, and spleens of immunized mice or from in vitro cultures were analyzed by ICS as previously described (Kim et al., 2017b). Prepared cells were restimulated with 50 ng/ml PMA (Sigma-Aldrich) and 500 ng/ml ionomycin (Sigma-Aldrich) for 5 h at 37°C in a humidified 5% CO_2 atmosphere. After stimulation, the cells were stained with Fixable Viability Dye (Invitrogen) against cell surface proteins, APC-eFluor780–conjugated anti-CD8, PE-Cy7–conjugated anti-CD4, and AF700-conjugated anti-CD44 antibodies (Thermo Fisher Scientific). Following surface staining, samples were fixed and permeabilized using the Intracellular Fixation & Permeabilization buffer Set (Thermo Fisher Scientific). After fixation and permeabilization, the cells were stained with antibodies against FITC-labeled anti–IFN-γ (BD Bioscience), PE-labeled anti–IL-4 (BD Bioscience), and APC-labeled anti–IL-17A (Thermo Fisher Scientific). Appropriate fluorescein-conjugated and isotype-matched monoclonal antibodies were used as isotype controls. Flow cytometry was performed with either MACSQuant Analyzer 10 (Miltenyi Biotec) or LSR Fortessa (BD Biosciences), and data were analyzed with FlowJo software (BD Biosciences).

Flow cytometry–based phospho-STAT5 assay
In 24-well plates, naive CD4+ T cells were cultured for 15 or 30 min in the presence of anti-CD3 and anti-CD28 antibodies. For phospho-STAT5 staining, cells were washed extensively before the addition of 20 ng/ml recombinant mIL-2 (BD Biosciences) and incubated at 37°C for 10, 15, or 30 min. Stimulated cells were collected at indicated time points and stained with an APC-conjugated anti–phospho-STAT5 monoclonal antibody according to the manufacturer's protocol C (Thermo Fisher Scientific). Additional surface staining was performed with APC-eFluor780–conjugated anti-CD8 (Thermo Fisher Scientific), PE-Cy7–conjugated anti-CD4 (Thermo Fisher Scientific), and live/dead cell viability staining. Intracellularly stained cells were analyzed using a MACSQuant Analyzer 10 (Miltenyi Biotec).

Immunocytochemistry
Cells were harvested and resuspended in ice-cold PBS. The resuspended cells were loaded into cytology funnel chambers and spun for 5 min at 400 rpm in a cytospin centrifuge to deposit a layer of cells on a microscope slide. Cytospin preparations were fixed with 3% paraformaldehyde, washed with PBS, and permeabilized in PBS containing 0.25% Triton X-100 (Sigma-Aldrich) for 10 min. Cells were incubated with anti-CD4 and anti–phospho-STAT5 (Cell Signaling) antibodies for 30 min, rinsed in PBS for 30 min, and incubated with FITC-conjugated and Texas red–conjugated secondary antibodies for 1 h. After 30 min of rinsing, 50 ml of a mounting solution containing DAPI (Abcam) was loaded on the cells, and a coverslip was slowly lowered to seal it. Images were acquired using a fluorescence microscope with ApoTome Technology (BX51; Olympus).

Confocal microscopy
Purified LN-TRCs were cultured on a microscope slide in a 6-well plate ($1 × 10^5$/well). The next day, $1 × 10^6$ naive CD4+ T cells from dsRed mice were loaded on the cultured LN-TRCs. rIL-2 (20 ng/ml) was added to each well and incubated for 1 h. After a light wash, cells were fixed with 1% paraformaldehyde and gently washed with PBS. After blocking with 5% donkey serum for 1 h, cells were stained with anti-gp38 and anti–IL-2 antibodies at 4°C overnight. After washing with PBS for 30 min, FITC-conjugated gp38 and Cy5-conjugated IL-2 secondary antibodies were stained for 1 h at room temperature. After 30 min washing with PBS, DAPI was loaded onto the cells. Fluorescence at 488, 594, and 647 nm was used for gp38, dsRed (CD4+ T cell), and IL-2, respectively. Images were acquired using LSM800 (Carl Zeiss).

PLA
LN-TRCs ($2 × 10^4$) purified from WT or CD25-deficient ($CD25^{fl/fl}CCL19^{cre}$) mice were cultured on glass coverslips

coated with poly-L-lysine (0.1 mg/ml; Sigma-Aldrich) in a 24-well plate. After TRC adhesion, 1×10^5 CD4^{+} T cells from healthy mice and rIL-2 (20 ng/ml) were loaded on the cultured LN-TRCs. After 1 h incubation, cells were fixed with 10% formalin for 10 min at room temperature, and PLA was performed to visualize IL-2–CD25 complexes on TRCs. Anti-CD25 (1:100; MyBioSource) and anti–IL-2 (1:50; Santa Cruz) primary antibodies were used, and then ligation and amplification of PLA were performed according to the manufacturer's instructions (Duolink In situ Red Kit; Sigma-Aldrich). After PLA, fluorescence of IL-2–CD25 complexes was detected on a confocal microscope (Olympus FV-1000) equipped with a 40×/0.95-NA oil-immersion objective and excitation/emission wavelength of 358/461 nm (DAPI) or 594/624 nm (Texas Red).

EAE induction
EAE was induced in the BMT, adoptively transferred, and specific gene–deleted group by immunization with a 200-mg MOG$_{35–55}$ peptide (MEVGWYRSPFSRVVHLYRNGK) emulsified in complete Freund's adjuvant (CFA; Sigma-Aldrich). The emulsion was injected s.c. into two sites in the flanks near the tail. On days 0 and 2, the immunized mice received additional i.p. injections of 200 ng pertussis toxin (List Biological Labs). Starting 1 wk after the first immunization, EAE phenotypes were scored daily as follows: 0, normal; 1, limp tail; 2, limp tail and partial paralysis of hind legs; 3, limp tail and complete paralysis of hind legs; 4 limp tail, complete paralysis of hind legs, and partial front leg paralysis; and 5, dead.

Aldara/IMQ-induced psoriasis
For induction of Aldara/IMQ-induced psoriasis, 62.5 mg of IMQ cream (5%; Aldara; 3M Pharmaceuticals) was applied daily on the shaved back of mice each day for 6 d. The score and the severity of inflammation including redness, scaling, and thickness were evaluated daily using a psoriasis area and severity index scale of 0–4 (0, none; 1, slight; 2, moderate; 3 marked; and 4, very marked). The cumulative score was calculated as the sum of the previous three scores (scale 0–12). In addition, epidermal thickness was measured daily using dial thickness gauge calipers (Peacock G; Ozaki MFG). On day 7, mice were sacrificed, and sections of paraffin-embedded skin tissue were stained with H&E.

AIA induction
Mice were immunized s.c. with 200 µg of methylated BSA (mBSA; Sigma-Aldrich) emulsified in 2 mg/ml of CFA (Sigma-Aldrich) in equal volumes. 7 d after initial immunization, 100 µg mBSA dissolved in 10 µl PBS was injected in the left knee intra-articularly to induce inflammation, and an identical volume of PBS was administered into the control right knee. On day 14, cells from iLNs were isolated and restimulated with 50 µg mBSA for ICS analysis. The severity of inflammatory arthritis was evaluated by histopathologic staining with H&E on sections of paraffin-embedded knee-joint tissue. Infiltration of inflammatory cells into synovium and joints were scored from 0 (normal) to 3 (severe).

Statistical analysis
Data are presented as a mean ± SEM and were analyzed with Prism software v9.0 for Windows (GraphPad). Significance

expressed as P values was compared with nonparametric Mann–Whitney U test, with 95% confidence intervals. *, $P < 0.05$; **, $P < 0.01$; and ***, $P < 0.001$ were applied.

Online supplemental material
Fig. S1 shows enhancement of proliferation and activation of CD4^{+} T cells by LN-TRCs regardless of CD25 expression. Fig. S2 describes expression of cytokine receptors on TRCs. Fig. S3 provides effects of coculture with WT or CD25-deficient TRCs on survival, proliferation, and activation of CD4^{+} T cells. Fig. S4 contains enhanced EAE phenotypes as a result of CD25 deficiency in TRCs. Fig. S5 details the CD4 T cell–mediated immune responses in CCL19[cre] and CD25^{fl/fl}CCL19[cre] mice after EAE induction. Table S1 describes the material resources.

References
Acton, S.E., J.L. Astarita, D. Malhotra, V. Lukacs-Kornek, B. Franz, P.R. Hess, Z. Jakus, M. Kuligowski, A.L. Fletcher, K.G. Elpek, et al. 2012. Podoplanin-rich stromal networks induce dendritic cell motility via activation of the C-type lectin receptor CLEC-2. Immunity. 37:276–289. https://doi.org/10.1016/j.immuni.2012.05.022

Alt, C., M. Laschinger, and B. Engelhardt. 2002. Functional expression of the lymphoid chemokines CCL19 (ELC) and CCL 21 (SLC) at the blood-brain barrier suggests their involvement in G-protein-dependent lymphocyte recruitment into the central nervous system during experimental autoimmune encephalomyelitis. Eur. J. Immunol. 32:2133–2144. https://doi.org/10.1002/1521-4141(200208)32:8<2133::aid-immu2133>3.0.co;2-w

Bajenoff, M., J.G. Egen, L.Y. Koo, J.P. Laugier, F. Brau, N. Glaichenhaus, and R.N. Germain. 2006. Stromal cell networks regulate lymphocyte entry, migration, and territoriality in lymph nodes. Immunity. 25:989–1001. https://doi.org/10.1016/j.immuni.2006.10.011

Kim et al.
LN-TRC–mediated T cell regulation

Journal of Experimental Medicine
https://doi.org/10.1084/jem.20200795

14 of 16

Bamford, R.N., A.J. Grant, J.D. Burton, C. Peters, G. Kurys, C.K. Goldman, J. Brennan, E. Roessler, and T.A. Waldmann. 1994. The interleukin (IL) 2 receptor beta chain is shared by IL-2 and a cytokine, provisionally designated IL-T, that stimulates T-cell proliferation and the induction of lymphokine-activated killer cells. *Proc. Natl. Acad. Sci. USA.* 91: 4940–4944. https://doi.org/10.1073/pnas.91.11.4940

Boyman, O., and J. Sprent. 2012. The role of interleukin-2 during homeostasis and activation of the immune system. *Nat. Rev. Immunol.* 12:180–190. https://doi.org/10.1038/nri3156

Bush, K.A., K.M. Farmer, J.S. Walker, and B.W. Kirkham. 2002. Reduction of joint inflammation and bone erosion in rat adjuvant arthritis by treatment with interleukin-17 receptor IgG1 Fc fusion protein. *Arthritis Rheum.* 46:802–805. https://doi.org/10.1002/art.10173

Chai, Q., L. Onder, E. Scandella, C. Gil-Cruz, C. Perez-Shibayama, J. Cupovic, R. Danuser, T. Sparwasser, S.A. Luther, V. Thiel, et al. 2013. Maturation of lymph node fibroblastic reticular cells from myofibroblastic precursors is critical for antiviral immunity. *Immunity.* 38:1013–1024. https://doi.org/10.1016/j.immuni.2013.03.012

Chirifu, M., C. Hayashi, T. Nakamura, S. Toma, T. Shuto, H. Kai, Y. Yamagata, S.J. Davis, and S. Ikemizu. 2007. Crystal structure of the IL-15-IL-15Ralpha complex, a cytokine-receptor unit presented in trans. *Nat. Immunol.* 8:1001–1007. https://doi.org/10.1038/ni1492

Cohen, J.N., C.J. Guidi, E.F. Tewalt, H. Qiao, S.J. Rouhani, A. Ruddell, A.G. Farr, K.S. Tung, and V.H. Engelhard. 2010. Lymph node-resident lymphatic endothelial cells mediate peripheral tolerance via Aire-independent direct antigen presentation. *J. Exp. Med.* 207:681–688. https://doi.org/10.1084/jem.20092465

Cote-Sierra, J., G. Foucras, L. Guo, L. Chiodetti, H.A. Young, J. Hu-Li, J. Zhu, and W.E. Paul. 2004. Interleukin 2 plays a central role in Th2 differentiation. *Proc. Natl. Acad. Sci. USA.* 101:3880–3885. https://doi.org/10.1073/pnas.0400339101

Dubois, S., J. Mariner, T.A. Waldmann, and Y. Tagaya. 2002. IL-15Ralpha recycles and presents IL-15 in trans to neighboring cells. *Immunity.* 17: 537–547. https://doi.org/10.1016/s1074-7613(02)00429-6

Dubrot, J., F.V. Duraes, L. Potin, F. Capotosti, D. Brighouse, T. Suter, S. LeibundGut-Landmann, N. Garbi, W. Reith, M.A. Swartz, and S. Hugues. 2014. Lymph node stromal cells acquire peptide-MHCII complexes from dendritic cells and induce antigen-specific CD4+ T cell tolerance. *J. Exp. Med.* 211:1153–1166. https://doi.org/10.1084/jem.20132000

Eicher, D.M., and T.A. Waldmann. 1998. IL-2R alpha on one cell can present IL-2 to IL-2R beta/gamma(c) on another cell to augment IL-2 signaling. *J. Immunol.* 161:5430–5437

Fletcher, A.L., V. Lukacs-Kornek, E.D. Reynoso, S.E. Pinner, A. Bellemare-Pelletier, M.S. Curry, A.R. Collier, R.L. Boyd, and S.J. Turley. 2010a. Lymph node fibroblastic reticular cells directly present peripheral tissue antigen under steady-state and inflammatory conditions. *J. Exp. Med.* 207:689–697. https://doi.org/10.1084/jem.20092642

Fletcher, J.M., S.J. Lalor, C.M. Sweeney, N. Tubridy, and K.H.G. Mills. 2010b. T cells in multiple sclerosis and experimental autoimmune encephalomyelitis. *Clin. Exp. Immunol.* 162:1–11. https://doi.org/10.1111/j.1365-2249.2010.04143.x

Gardner, J.M., J.J. Devoss, R.S. Friedman, D.J. Wong, Y.X. Tan, X. Zhou, K.P. Johannes, M.A. Su, H.Y. Chang, M.F. Krummel, and M.S. Anderson. 2008. Deletional tolerance mediated by extrathymic Aire-expressing cells. *Science.* 321:843–847. https://doi.org/10.1126/science.1159407

Gillis, S., and K.A. Smith. 1977. Long term culture of tumour-specific cytotoxic T cells. *Nature.* 268:154–156. https://doi.org/10.1038/268154a0

Glegg, R.E., D. Eidinger, and C.P. Leblond. 1953. Some carbohydrate components of reticular fibers. *Science.* 118:614–616. https://doi.org/10.1126/science.118.3073.614

Granucci, F., C. Vizzardelli, N. Pavelka, S. Feau, M. Persico, E. Virzi, M. Rescigno, G. Moro, and P. Ricciardi-Castagnoli. 2001. Inducible IL-2 production by dendritic cells revealed by global gene expression analysis. *Nat. Immunol.* 2:882–888. https://doi.org/10.1038/ni0901-882

Gretz, J.E., E.P. Kaldjian, A.O. Anderson, and S. Shaw. 1996. Sophisticated strategies for information encounter in the lymph node: The reticular network as a conduit of soluble information and a highway for cell traffic. *J. Immunol.* 157:495–499

Gunn, M.D., K. Tangemann, C. Tam, J.G. Cyster, S.D. Rosen, and L.T. Williams. 1998. A chemokine expressed in lymphoid high endothelial venules promotes the adhesion and chemotaxis of naive T lymphocytes. *Proc. Natl. Acad. Sci. USA.* 95:258–263. https://doi.org/10.1073/pnas.95.1.258

Ivanov, I.I., B.S. McKenzie, L Zhou, C.E. Tadokoro, A. Lepelley, J.J. Lafaille, D.J. Cua, and D.R. Littman. 2006. The orphan nuclear receptor RORgammat directs the differentiation program of proinflammatory IL-17+ T helper cells. *Cell.* 126:1121–1133. https://doi.org/10.1016/j.cell.2006.07.035

Katakai, T., T. Hara, M. Sugai, H. Gonda, and A. Shimizu. 2004. Lymph node fibroblastic reticular cells construct the stromal reticulum via contact with lymphocytes. *J. Exp. Med.* 200:783–795. https://doi.org/10.1084/jem.20040254

Kim, D.E., M.J. Jang, Y.R. Kim, J.Y. Lee, E.B. Cho, E. Kim, Y. Kim, M.Y. Kim, W.I. Jeong, S. Kim, et al. 2017a. Prediction of drug-induced immune-mediated hepatotoxicity using hepatocyte-like cells derived from human embryonic stem cells. *Toxicology.* 387:1–9. https://doi.org/10.1016/j.tox.2017.06.005

Kim, D.E., Y. Lee, M. Kim, S. Lee, S. Jon, and S.H. Lee. 2017b. Bilirubin nanoparticles ameliorate allergic lung inflammation in a mouse model of asthma. *Biomaterials.* 140:37–44. https://doi.org/10.1016/j.biomaterials.2017.06.014

Laurence, A., C.M. Tato, T.S. Davidson, Y. Kanno, Z. Chen, Z. Yao, R.B. Blank, F. Meylan, R. Siegel, L. Hennighausen, et al. 2007. Interleukin-2 signaling via STAT5 constrains T helper 17 cell generation. *Immunity.* 26: 371–381. https://doi.org/10.1016/j.immuni.2007.02.009

Le Gros, G., S.Z. Ben-Sasson, R. Seder, F.D. Finkelman, and W.E. Paul. 1990. Generation of interleukin 4 (IL-4)-producing cells in vivo and in vitro: IL-2 and IL-4 are required for in vitro generation of IL-4-producing cells. *J. Exp. Med.* 172:921–929. https://doi.org/10.1084/jem.172.3.921

Leonard, W.J., K. Imada, H. Nakajima, A. Puel, E. Soldaini, and S. John. 1999. Signaling via the IL-2 and IL-7 receptors from the membrane to the nucleus. *Cold Spring Harb Symp. Quant Biol.* 64:417–424. https://doi.org/10.1101/sqb.1999.64.417

Liao, W., J.X. Lin, L. Wang, P. Li, and W.J. Leonard. 2011. Modulation of cytokine receptors by IL-2 broadly regulates differentiation into helper T cell lineages. *Nat. Immunol.* 12:551–559. https://doi.org/10.1038/ni.2030

Link, A., T.K. Vogt, S. Favre, M.R. Britschgi, H. Acha-Orbea, B. Hinz, J.G. Cyster, and S.A. Luther. 2007. Fibroblastic reticular cells in lymph nodes regulate the homeostasis of naive T cells. *Nat. Immunol.* 8: 1255–1265. https://doi.org/10.1038/ni1513

Lukacs-Kornek, V., D. Malhotra, A.L. Fletcher, S.E. Acton, K.G. Elpek, P. Tayalia, A.R. Collier, and S.J. Turley. 2011. Regulated release of nitric oxide by nonhematopoietic stroma controls expansion of the activated T cell pool in lymph nodes. *Nat. Immunol.* 12:1096–1104. https://doi.org/10.1038/ni.2112

Malhotra, D., A.L. Fletcher, J. Astarita, V. Lukacs-Kornek, P. Tayalia, S.F. Gonzalez, K.G. Elpek, S.K. Chang, K. Knoblich, M.E. Hemler, et al. 2012. Transcriptional profiling of stroma from inflamed and resting lymph nodes defines immunological hallmarks. *Nat. Immunol.* 13:499–510. https://doi.org/10.1038/ni.2262

Minami, Y., T. Kono, T. Miyazaki, and T. Taniguchi. 1993. The IL-2 receptor complex: Its structure, function, and target genes. *Annu. Rev. Immunol.* 11:245–268. https://doi.org/10.1146/annurev.iy.11.040193.001333

Morgan, D.A., F.W. Ruscetti, and R. Gallo. 1976. Selective in vitro growth of T lymphocytes from normal human bone marrows. *Science.* 193:1007–1008. https://doi.org/10.1126/science.181845

Mueller, S.N., and R.N. Germain. 2009. Stromal cell contributions to the homeostasis and functionality of the immune system. *Nat. Rev. Immunol.* 9:618–629. https://doi.org/10.1038/nri2588

Nakamura, Y., S.M. Russell, S.A. Mess, M. Friedmann, M. Erdos, C. Francois, Y. Jacques, S. Adelstein, and W.J. Leonard. 1994. Heterodimerization of the IL-2 receptor beta- and gamma-chain cytoplasmic domains is required for signalling. *Nature.* 369:330–333. https://doi.org/10.1038/369330a0

Owen, D.L., S.A. Mahmud, K.B. Vang, R.M. Kelly, B.R. Blazar, K.A. Smith, and M.A. Farrar. 2018. Identification of cellular sources of IL-2 needed for regulatory T cell development and homeostasis. *J. Immunol.* 200: 3926–3933. https://doi.org/10.4049/jimmunol.1800097

Parsonage, G., A. Filer, M. Bik, D. Hardie, S. Lax, K. Howlett, L.D. Church, K. Raza, S.H. Wong, E. Trebilcock, et al. 2008. Prolonged, granulocyte-macrophage colony-stimulating factor-dependent, neutrophil survival following rheumatoid synovial fibroblast activation by IL-17 and TNFalpha. *Arthritis Res. Ther.* 10:R47. https://doi.org/10.1186/ar2406

Sarkar, S., L.A. Cooney, and D.A. Fox. 2010. The role of T helper type 17 cells in inflammatory arthritis. *Clin. Exp. Immunol.* 159:225–237. https://doi.org/10.1111/j.1365-2249.2009.04016.x

Saxena, V., L. Li, C. Paluskievicz, V. Kasinath, A. Bean, R. Abdi, C.M. Jewell, and J.S. Bromberg. 2019. Role of lymph node stroma and microenvironment in T cell tolerance. *Immunol. Rev.* 292:9–23. https://doi.org/10.1111/imr.12799

Schluns, K.S., and L. Lefrancois. 2003. Cytokine control of memory T-cell development and survival. *Nat. Rev. Immunol.* 3:269–279. https://doi.org/10.1038/nri1052

Setoguchi, R., S. Hori, T. Takahashi, and S. Sakaguchi. 2005. Homeostatic maintenance of natural Foxp3+ CD25+ CD4+ regulatory T cells by interleukin (IL)-

2 and induction of autoimmune disease by IL-2 neutralization. *J. Exp. Med.* 201:723–735. https://doi.org/10.1084/jem.20041982

Shi, M., T.H. Lin, K.C. Appell, and L.J. Berg. 2008. Janus-kinase-3-dependent signals induce chromatin remodeling at the Ifng locus during T helper 1 cell differentiation. *Immunity.* 28:763–773. https://doi.org/10.1016/j.immuni.2008.04.016

Sixt, M., N. Kanazawa, M. Selg, T. Samson, G. Roos, D.P. Reinhardt, R. Pabst, M.B. Lutz, and L. Sorokin. 2005. The conduit system transports soluble antigens from the afferent lymph to resident dendritic cells in the T cell area of the lymph node. *Immunity.* 22:19–29. https://doi.org/10.1016/j.immuni.2004.11.013

Stoll, S., J. Delon, T.M. Brotz, and R.N. Germain. 2002. Dynamic imaging of T cell-dendritic cell interactions in lymph nodes. *Science.* 296:1873–1876. https://doi.org/10.1126/science.1071065

Sutton, C., C. Brereton, B. Keogh, K.H. Mills, and E.C. Lavelle. 2006. A crucial role for interleukin (IL)-1 in the induction of IL-17-producing T cells that mediate autoimmune encephalomyelitis. *J. Exp. Med.* 203:1685–1691. https://doi.org/10.1084/jem.20060285

Tesmer, L.A., S.K. Lundy, S. Sarkar, and D.A. Fox. 2008. Th17 cells in human disease. *Immunol. Rev.* 223:87–113. https://doi.org/10.1111/j.1600-065X.2008.00628.x

Volin, M.V., and S. Shahrara. 2011. Role of TH-17 cells in rheumatic and other autoimmune diseases. *Rheumatology (Sunnyvale).* 1:2169. https://doi.org/10.4172/2161-1149.1000104

Waite, J.C., and D. Skokos. 2012. Th17 response and inflammatory autoimmune diseases. *Int. J. Inflamm.* 2012:819467. https://doi.org/10.1155/2012/819467

Wang, X., M. Rickert, and K.C. Garcia. 2005. Structure of the quaternary complex of interleukin-2 with its alpha, beta, and gammac receptors. *Science.* 310:1159–1163. https://doi.org/10.1126/science.1117893

Wuest, S.C., J.H. Edwan, J.F. Martin, S. Han, J.S. Perry, C.M. Cartagena, E. Matsuura, D. Maric, T.A. Waldmann, and B. Bielekova. 2011. A role for interleukin-2 trans-presentation in dendritic cell-mediated T cell activation in humans, as revealed by daclizumab therapy. *Nat. Med.* 17:604–609. https://doi.org/10.1038/nm.2365

Wulfing, C., M.D. Sjaastad, and M.M. Davis. 1998. Visualizing the dynamics of T cell activation: Intracellular adhesion molecule 1 migrates rapidly to the T cell/B cell interface and acts to sustain calcium levels. *Proc. Natl. Acad. Sci. USA.* 95:6302–6307. https://doi.org/10.1073/pnas.95.11.6302

Yamane, H., and W.E. Paul. 2012. Cytokines of the γ(c) family control CD4+ T cell differentiation and function. *Nat. Immunol.* 13:1037–1044. https://doi.org/10.1038/ni.2431

Yang, J., M.S. Sundrud, J. Skepner, and T. Yamagata. 2014. Targeting Th17 cells in autoimmune diseases. *Trends Pharmacol. Sci.* 35:493–500. https://doi.org/10.1016/j.tips.2014.07.006

Yoo, S.A., M. Kim, M.C. Kang, J.S. Kong, K.M. Kim, S. Lee, B.K. Hong, G.H. Jeong, J. Lee, M.G. Shin, et al. 2019. Placental growth factor regulates the generation of TH17 cells to link angiogenesis with autoimmunity. *Nat. Immunol.* 20:1348–1359. https://doi.org/10.1038/s41590-019s4150456-4

Zaffran, Y., O. Destaing, A. Roux, S. Ory, T. Nheu, P. Jurdic, C. Rabourdin-Combe, and A.L. Astier. 2001. CD46/CD3 costimulation induces morphological changes of human T cells and activation of Vav, Rac, and extracellular signal-regulated kinase mitogen-activated protein kinase. *J. Immunol.* 167:6780–6785. https://doi.org/10.4049/jimmunol.167.12.6780

Zhu, J., H. Yamane, and W.E. Paul. 2010. Differentiation of effector CD4 T cell populations (*). *Annu. Rev. Immunol.* 28:445–489. https://doi.org/10.1146/annurev-immunol-030409-101212
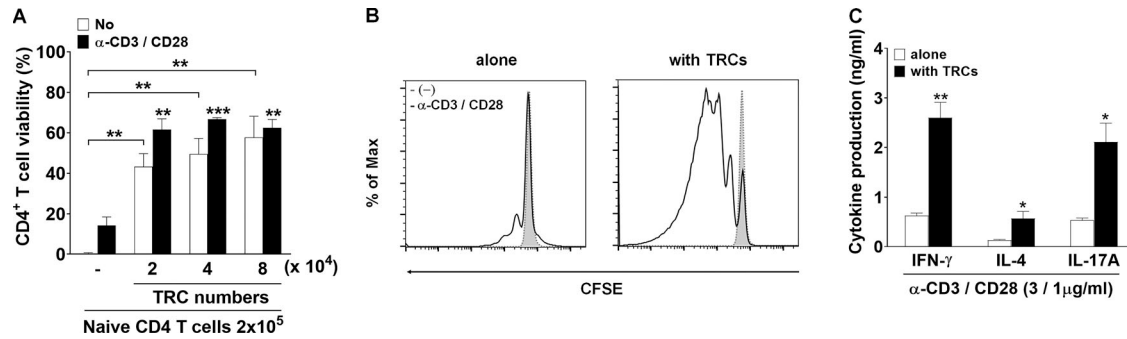
Figure S1. **Enhancement of proliferation and activation of CD4+ T cells by LN-TRCs regardless of CD25 expression. (A)** Naive CD4+ T cells (2×10^5) were cultured for 72 h with or without TRCs (ratio of T cells to TRCs is 10:1, 5:1, and 2.5:1) and treated with (black bars) or without (white bars) anti-CD3 and CD28 antibodies (3 and 1 µg/ml) to stimulate T cells with irradiated splenocytes as APCs (2×10^5). Cell viability was assessed by flow cytometry with viability dye staining. **, P < 0.01; ***, P < 0.001 compared with naive CD4+ T cells in the absence of stimulation or antibody stimulation. Error bars indicate the mean ± SEM (n = 4 per each group). **(B)** Comparison of the proliferation of CFSE-labeled naive CD4+ T cells (2×10^5) cultured for 72 h with or without TRCs (2×10^4) in the presence or absence of anti-CD3 and CD28 antibodies (3 and 1 µg/ml) with irradiated APCs (2×10^5). The proliferation of CFSE-labeled naive CD4+ T cells was analyzed by flow cytometry (1×10^5). **(C)** The production of cytokines in supernatants naive CD4+ T cells (2×10^5) cultured for 72 h with (black bars) or without (white bars) TRCs (2×10^4) in the presence of anti-CD3 and CD28 antibodies (3 and 1 µg/ml) with irradiated APCs (2×10^5) was quantified in the culture supernatants by ELISA. *, P < 0.05; **, P < 0.01 compared with naive CD4+ T cells in the absence of stimulation or antibody-stimulated CD4+ T cells. Error bars indicate the mean ± SEM (n = 4 per each group). Data are representative of three independent experiments.
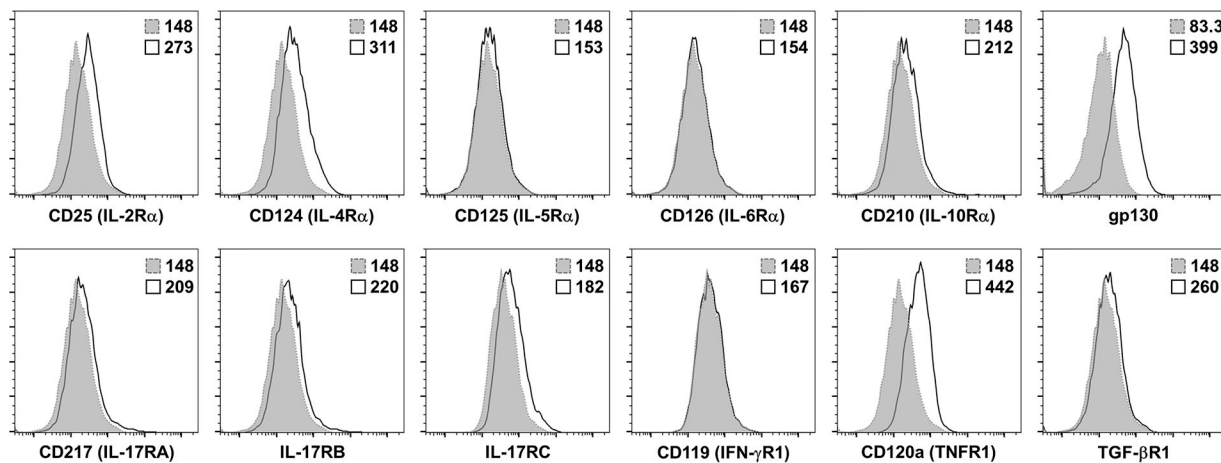

Figure S2. **Expression of cytokine receptors on TRCs.** Expression of cytokine receptors on sorted LN-TRCs was analyzed with antibodies against CD25, CD124, CD125, CD126, CD210, gp130, CD217, IL-17RB, IL-17RC, CD119, CD120a, and TGF-βR1 (solid lines) or fluorescence minus one (shaded with dotted lines). Data are representative of three independent experiments.
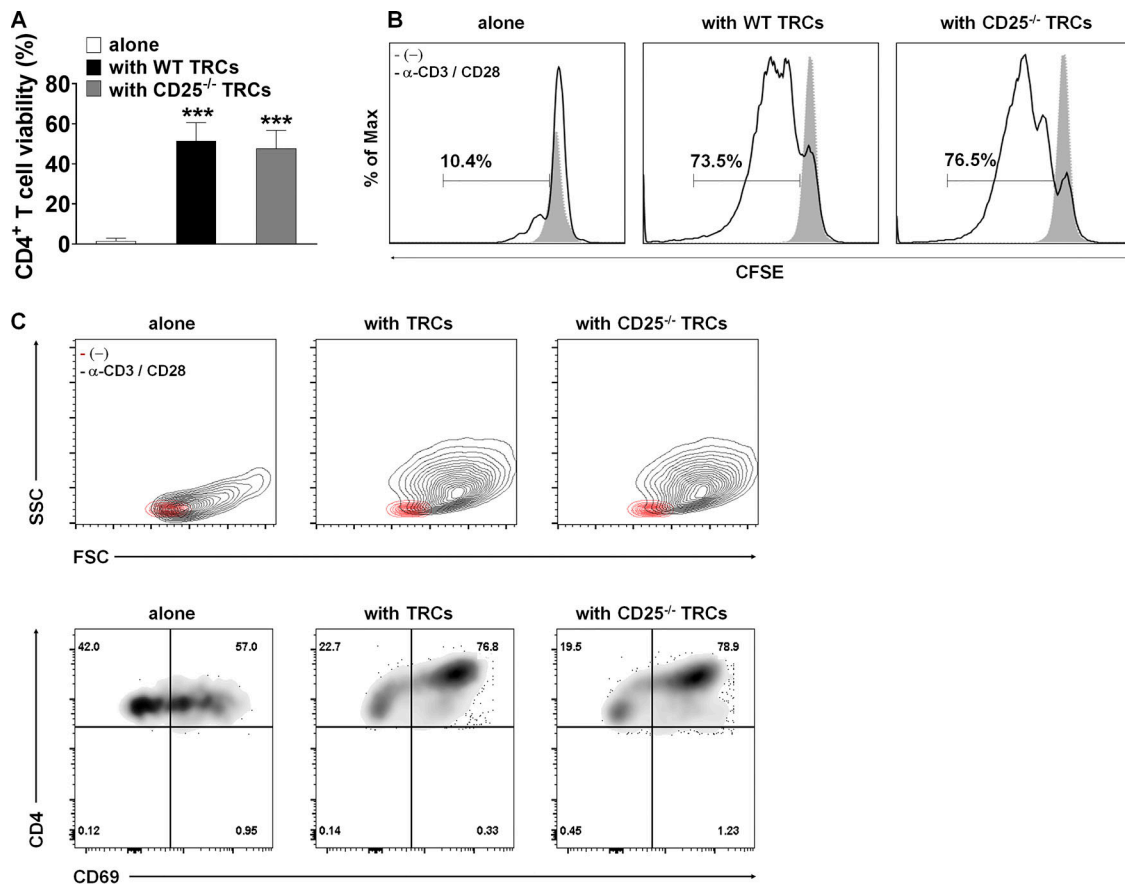
Figure S3. **Effects of coculture with WT or CD25-deficient TRCs on survival, proliferation, and activation of CD4+ T cells.** Purified, CFSE-labeled naive CD4+ T cells (2×10^5) were cultured without or with either WT or CD25-deficient TRCs (2×10^4) in the presence or absence of soluble anti-CD3 and CD28 antibodies (3 and 1 µg/ml) with irradiated APCs (2×10^5) for 72 h. **(A)** Cell viability was assessed by FACS analysis with viability dye staining. ***, P < 0.001 compared with naive CD4+ T cells alone. Error bars indicate the mean ± SEM ($n \geq 5$ per group). **(B)** The proliferation of CFSE-labeled CD4+ T cells was measured by FACS analysis. **(C)** Representative flow cytometric analysis of FSC/SSC and CD4+/CD69+ cell profiles. Data are representative of three independent experiments.
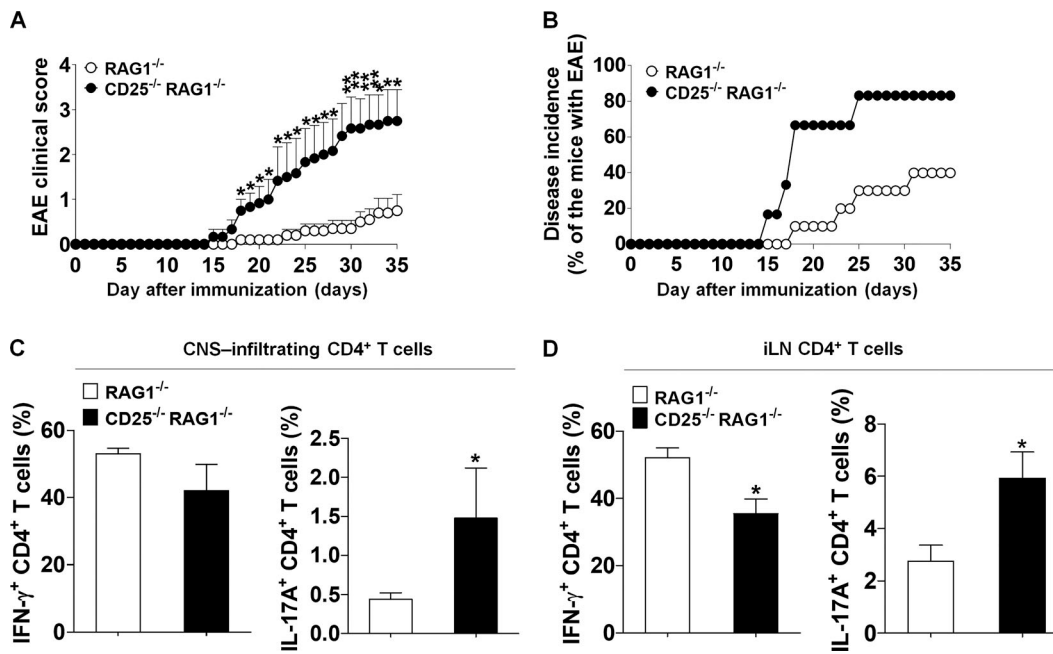
Figure S4. Enhanced EAE phenotypes as a result of CD25 deficiency in TRCs. Reconstituted mice were immunized with MOG_{35-55}, CFA, and pertussis toxin to induce EAE ($RAG1^{-/-}$, $n = 10$; or $CD25^{-/-}RAG1^{-/-}$, $n = 6$). **(A)** The mean clinical scores representing disease severity were observed for the indicated times. *, $P < 0.05$; **, $P < 0.01$ compared with RAG1-deficient EAE-induced mice. Error bars indicate the mean ± SEM. **(B)** Disease incidence was assessed at the indicated times. **(C and D)** IFN-γ⁺ or IL-17A⁺ CD4⁺ T cell populations were analyzed by flow cytometry and quantified in CNS (C) or iLN (D) populations. *, $P < 0.05$ compared with RAG1-deficient EAE-induced mice. Error bars indicate the mean ± SEM. Data are representative of three independent experiments.
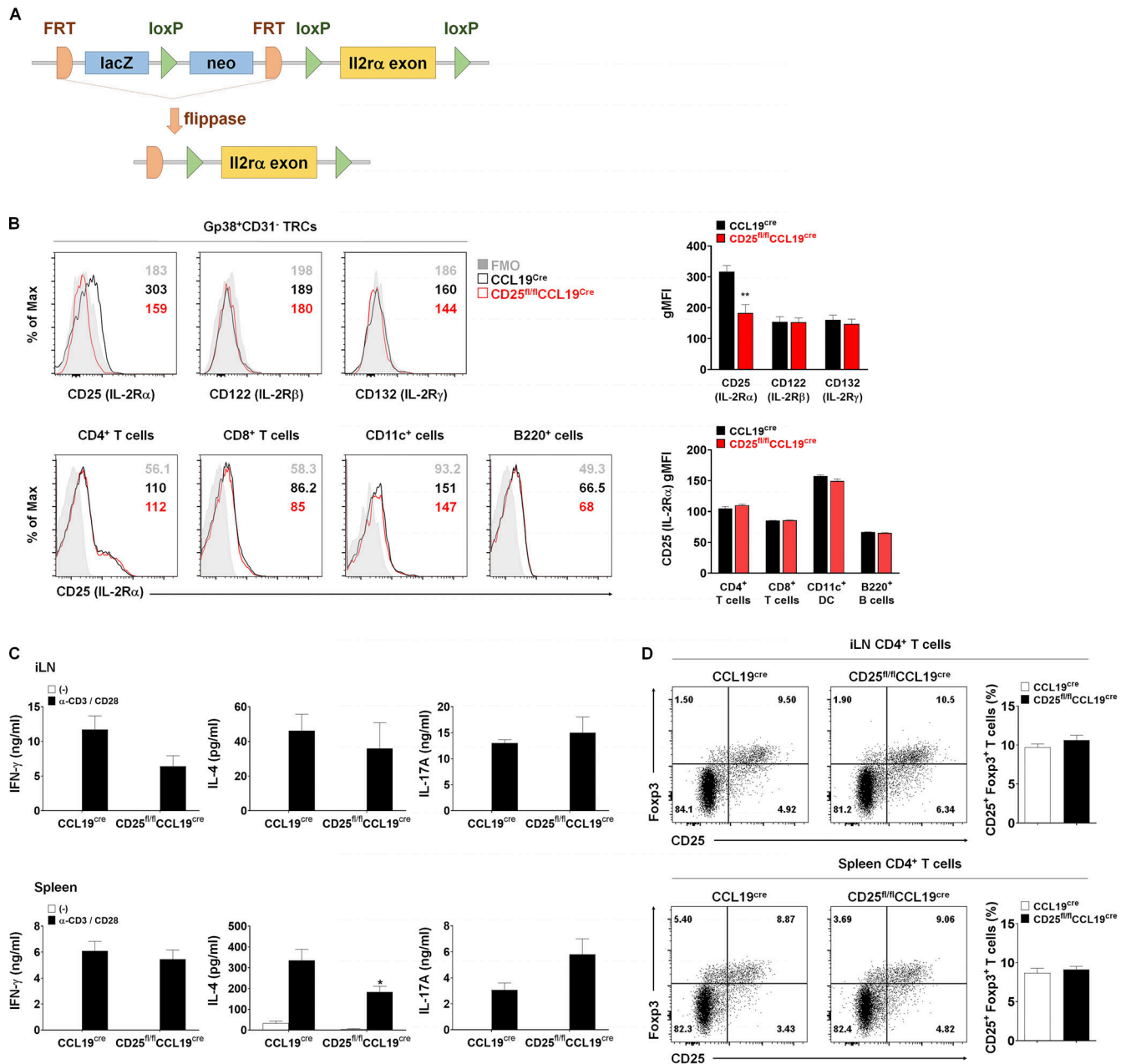
Figure S5. **CD4 T cell–mediated immune responses in CCL19cre and CD25fl/flCCL19cre mice after EAE induction. (A)** Targeting of the IL2rα (CD25) locus. **(B)** The expression of CD25, CD122, and CD132 on CD31−gp38+ TRCs from freshly isolated iLNs of CCL19cre (black bars) or CD25fl/flCCL19cre (red bars) mice was measured by flow cytometry (top). The expression of CD25 on CD4+ T cells, CD8+ T cells, CD11c+ DCs, and B220+ B cells from spleens of CCL19cre (black bars) or CD25fl/flCCL19cre (red bars) mice was measured by flow cytometry (bottom). Gray histograms represent fluorescence minus one (FMO) control. **, P < 0.01 compared with the CCL19cre mice. Error bars indicate the mean ± SEM (n = 6). **(C)** Measurement of cytokine production in culture supernatants from re-stimulated iLN cells and splenocytes by ELISA. * P < 0.05 compared with the CCL19cre EAE-induced control group. Error bars indicate the mean ± SEM (n ≥ 6 per group). **(D)** Representative and compiled data of Foxp3+CD25+ regulatory T (Treg) cells in CD4+ T cells as assessed by flow cytometric analysis of iLNs and spleens. Error bars indicate the mean ± SEM (n ≥ 6 per group). Data are representative of three independent experiments.

Provided online is one table. Table S1 describes the material resources.